Stability Study of Bilateral Tele-operation Systems with Haptic Device

Lingfang Dong

A Thesis

in

The department

of

Electrical and Computer Engineering

Presented in Partial Fulfillment of the Requirements for

the Degree of Master of Applied Science

(Electrical and Computer Engineering) at

Concordia University

Montreal, Quebec, Canada

February 2006

Your file Votre référence
ISBN: 978-0-494-20743-7
Our file Notre référence
ISBN: 978-0-494-20743-7

Abstract

Stability Study of Bilateral Tele-operation Systems with Haptic Devices

Lingfang Dong

Tele-operation has been a hot topic for a long time in computer science and electrical engineering fields since it has been applied in many different domains such as dangerous operating environments, deep-sea operations, and multiple operations through network. At the same time, bilateral control technology has resulted in significant interests by people, since information such as force reflection will improve the perception of the operator to interact with environment with great capabilities. As a result, stability of bilateral systems is of particular importance as unstable force reflection could hurt the human operator.

However, in tele-operation systems, time delay always exists and it varies with the network performance, and this time delay, even very small, will destabilize an originally stable system. That is why that stability problem is so important and critical in the tele-operation bilateral systems. This is the main motivation for this thesis research.

In this thesis, wave transfer method is investigated and introduced into the stability and control of bilateral tele-operation systems. However, using a wave variable tele-operation system with a PD controller to maintain the position tracking of the slave side has resulted in undesired position drifts.

Sliding mode control is an effective robust control method and is particularly useful for solving tracking problems. The control objective is to force the system dynamics approach to the sliding surface and remain on it for all the future time to

eliminate or minimize the tracking errors. Consequently, the designed sliding-mode controller as validated and verified in the simulation results decreases the tracking error and guarantees the slave track the master position quite satisfactorily for bilateral tele-operation system with varying time delay.

The contribution of this thesis is the investigation of the model of the phantom haptic device and analysis of the tele-operation system using the phantom device as master and slave manipulator. The designed wave variable sliding mode controller guarantees the stability of the tele-operation system having time varying communication delays.

Acknowledgements

I would like to express my extreme gratitude to Pro. K. Khorasani for his supervision. I have benefited greatly from his expertise, vision and conscientious attitude toward science during the conducting of this research. His constant support, great suggestions, and precious encouragement have played a crucial role in the development of this thesis.

I am greatly thankful to friends in our robotic control lab for sharing their smart idea and precious experience. Specially thanks to my family for their encouragement and all kinds of support. I am so proud to have parents who love me deeply and understand me thoroughly throughout my life.

TABLE OF CONTENT

List of Figures

Chapter 1

Introduction

Since its early use in remote manipulation of radioactive materials, tele-operation has extended its scope to include manipulation at different scales and lately in virtual world. Applications can be found in space and undersea [1], exploration and servicing [2], microsurgery and micro assembly [3], and computer user interfaces [4].

In tele-operation applications, an operator controls the action of a distant or inaccessible slave device by manipulating a master device, and the goal of tele-operation is to achieve transparency by mimicking human motor and sensory functions [5].

Although tele-operation has reached a considerable development from both a technological and conceptual point of view, there are still many problems that could not find a satisfactory solution. These problems can be summarized as follows [6].

1.1. Transparency Issues

One of the most important tele-operation characteristics is transparency. Transparency is achieved if the operator can manipulate the remote actual tool as he or she can do to the master device. The ability of a tele-operation system to provide transparency depends largely on the performance of the master device and interface. When this interface provides kinesthetic or tactile feedback to the user, it is called a haptic interface. Its performance depends on its electromechanical design and the algorithms used to control it.

Meeting stability and transparency requirement at the same time is a challenging issue in tele-operation field. Although there have been some solutions from a control theory point-of-view, ideal transparency is hard to be reached by conventional bilateral control. This is because the operator action and the feedback are transmitted through the master-slave chain before reaching the target task and the operator respectively and this chain includes dynamics which can not be neglected or compensated without stability or operator safety compromise.

If the operator manipulate a tool in the local site, he or she may have more sensory information such as visual, tactile, audio, and haptic cues. However, these sensory cues diminish when the operator manipulate a tool in remote site. When these cues are sensed through sensors at the remote site and then displayed to the operator, there is always some loss of information [7]. This loss occurs because the sensors do not pick up all the cues adequately and they cannot be completely reproduced for the operator.

1.2. Communication Bandwidth Issue

In tele-operation, communication between the master and the remote site is not ignorable. However, due to the location of the some remote site, some tele-operation tasks have to be performed in remote site which broad bandwidth telecommunication is not available. For example, tethered underwater robots are limited by their operating distance, and the cables tend to snag with underwater structures [8]. However, untethered communication channels have a limited or insufficient bandwidth.

However, lower bandwidth could diminish some sensory information from the remote site to operator. For instance, video signal transmission needs very high bandwidth. A lower bandwidth will cause dropping of display frame rate, and the visual quality of the display. In general, operator performance has been shown to be adversely affected by decreases in the frame rate, resolution and grayscale [9]. As for bilateral force feedback system, the lower bandwidth will increase the time delay, which could cause serous stability issue.

1.3. Continuous Manipulation Issue

Tele-operation flexibility depends on operator skillfulness to the tele-operation system. The manual control of remote manipulators requires sufficient training, before the operator becomes familiar with the dynamics of the system. Further substantial training is required for a coordinated manipulation of the remote system [10]. Many solutions concerning man-machine cooperation have been proposed. The problem of autonomy sharing, modeling and quantification is linked to the degree of robot autonomy and to the level of operator intervention.

Some remote manipulators can be very slow to respond because of their high inertia, or low acceleration of the manipulator, while in other systems the operator has to adopt a move-and-wait strategy because of high time delay. Manual control of the remote manipulator in such cases can be stressful if carried out for long periods of time, as the operator is continuously tied in the control loop. Also, low level of continuous involvement in the task can prevent the operator from doing higher level tasks, such as planning the next manipulation step.

1.4. Manipulation Safety and Error Issue

Using of powered haptic feedback devices is dangerous, since losses of functionality could happen. The haptic device have the physical capability of destroying themselves and their environments if used improperly.

One of the biggest concerns during tele-operation is that the manipulator should not collide with other objects in task space, to avoid damage to the manipulator or other objects in the task space. Also, damage might occur when the manipulator end-effector moves with very high velocity or when the manipulator exert excessive forces on the other objects when collision happens. In some cases the manipulator has to operate within the restrictions of a three dimensional envelope which should not be exceeded [11].

Tele-operation errors involve undesirable manipulations, such as mis-positioning of the end-effector, a hit and miss trial approach by the operator to achieve appropriate contact to an object, and slipping of an object which has been gripped by the manipulator. Also, mistakes occur due to incorrect interpretation of the remote environment or the task, or when an incorrect manipulation sequence is selected. Some of these tele-operation errors may be due to human error, such as mistakes and slips. Slips are accidental movements of the manipulator caused by the operator, while other errors could be due to the fact that the operator does not get sufficient feedback from the remote site.

1.5. Autonomy Issue

Autonomy in tele-operation system refers to the extent to which the remote manipulator can function independently of the human operator. It can be achieved if some part of control is achieved by a computer located at the remote site. The operator can thus provide higher levels of control to the remote computer, while the remote computer can execute the lower levels of control.

A fully autonomous tele-operation system which can successfully perform the remote task, and has the ability to sense and perceive the effects of its actions is unlikely to be realized in the near future [12]. So only partial autonomy in the system can be expected, with tasks allocated between the machine and human operator.

The allocation of tasks between humans and machines should be based on their respective strengths, capabilities and limitations. In general, humans are good at perception and understanding, task decomposition, problem solving, fault detection and replanning for fault recovery, while machines are better at low level sensory and control functions, trajectory planning, executing precise motion, information processing, performing routine and repetitive tasks, and handling complex operations involving many variables and fast control response [13]. Tele-operation reliability, efficiency and effectiveness can be improved if part of the task that is unsuitable for humans could be performed by an automated subsystem. In order to partially disengage the human operator from the control loop implies a certain level of autonomy from the computer at the remote site. Since such autonomous procedures are very limited in their capability in some environment, direct manual control are still necessary.

1.6. Time Delay Issue

A time delay in communication between local and remote site can occur due to a large distance between them, to a low speed of data transmission, or to computer processing at different stages. Time delay affects not only transparency but also stability, since the operator actions and feedback information are delayed which will be further discussed in Chapter 2.

Continuous manual control of the remote manipulator can be destroyed if there is a time delay between the control input by the operator and the consequent feedback of its control actions visible on the display. A continuous closed loop control becomes unstable when the time delay exists in the control loop. Ferrell [14] showed that when the human operator is in the control loop, this instability can be avoided by using a "move and wait strategy", where the operator makes small incremental moves in an open loop fashion and then waits for a new update of the position of the tele-robot.

Force feedback bilateral tele-operation is based on the perception that contact force information to the human operator can improve task performance. Although this information can be obtained from visual displays, it is more useful when provided directly, by reflecting the measured force to motors on the master side. When this is envolved, the contact force is said to be reflected to the human operator, and the tele-operator is said to be controlled bilaterally. When tele-operation is performed over a great distance, such as in undersea and outer space operations, a time delay is incurred in the transmission of information from one site to another. This time delay can destabilize a bilaterally controlled tele-operation.

1.7. Topics of Interest

As mentioned in section 1.1, a number of issues related to tele-operation technology are still outstanding, and researchers have performed a lot of work in each of these issues. However, in this thesis, we are more concerned about the time delay issue.

Time delay issue is quite important as time delay is a fact that one has to face when one deals with tele-operation, and it affects the system stability and human operation safety. In the case of bilateral tele-operation, commands are sent by the human operator through the local haptic device to the remote environment. The time delay between the local and the remote site could destabilize the system. It is shown [15] that it is unacceptable to feed resolved force continuously back to the same hand that is operating the control. This is because the delayed feedback imposes an unexpected disturbance on the hand which the operator cannot ignore and which, in turn, forces instability on the process.

A large volume of work has been performed to try to compensate this factor to stabilize the system. In Chapter 2, we will review some typical technologies which intend to solve the stability issue caused by time delay in tele-operation systems.

1.8. Thesis Objectives

The objective of this thesis is to design a control scheme to stabilize the tele-operation system, and at the same time ensures that the position of the slave device tracks that of the master device despite the existence of time delays in communication between the master and slave sides. Furthermore, analysis is provided for the tele-operation system with time varying delay, and validation of the control scheme is verified on the system with time varying delay.

1.9. Contributions of This Thesis

The contributions of this thesis are as follows:

1. Wave variable transformation and sliding mode control technolodge is integrated as a wave variable sliding mode control strategy to gurantee the stability and precise slave side tracking of the bilateral haptic feedback tele-operation system.
2. Nonlinear model of Phantom haptic feed back device is investigated based on the previous research work, and linearization of the model is performed. Further the controller is designed to stabilize the phantom haptic device itself.
3. Tele-operation system with Phantom haptic device at master and slave side is simulated, and the communication delay effects on this system are investigated.
4. The wave variable sliding mode control scheme is applied to the bilateral haptic tele-operation system with time varying delay established above and validation of this system is performed by simulations.

Chapter 2

Background Information

In this chapter, we will introduce some background information on tele-operation and virtual reality technologies. Characteristics of tele-operation applications will be reviewed in section 2.1, and virtual reality based tele-operation will be reviewed in section 2.2. In section 2.3, haptic device and its application will be presented in order to help the reader easily understand this field. The time delay issue, which is the main issue of concern in this thesis will be analyzed from the basic control knowledge in section 2.4. Furthermore, the current solutions to the time delay issue will be summarized, which

include Smith prediction method, Model based controller design and wave variable technology.

2.1 Characteristics of Tele-operation Systems [16], [17]

Tele-operation has some characteristics which are different from the usual robot systems due to the remote distance between the operator and the location where the tasks are performed. These characteristics can be summarized below.

2.1.1. Feedback Information from Remote Site

When a human operator is physically present at the site and perform physical manipulations directly, he or she could receive a variety of feedbacks of the result of his or her manipulations, such as visual, auditory, tactile, and force. In addition, he or she would be able to change his or her viewpoint to get better visual feedback. However when the human is remotely located from the task space and tries to perform some physical manipulation, the feedback of his or her control actions has to be transmitted back to him or her through a transmission channel. The relevant cues at the remote site are picked up by the sensors, sent to the operator's location and then reproduced to provide feedback [18].

The number of sensors and the types of cues which are sensed vary widely depending on the types of remote task. These sensor signals are transmitted through a communication link and displayed on the operator interface. For instance a video monitor shows the video signal and a force reflecting device provides forces experienced by the

robot arm. Based on this display, the operator decides how the tasks should be performed, plans the elemental manipulations needed to perform the task and applies control to an input device to move the robot arm.

2.1.2. Variety of Tele-operation Systems

Based on the nature of the task and its environment, tele-operation systems are designed to meet requirement of each task and vary widely in their design. However, in a typical configuration of a remote manipulation system, a manipulator or robot is sent to the remote site to do the task. Ideally, this manipulation system should have enough dexterity and flexibility, so that it can follow the manipulation commands given by the operator. To do this, there are sensors at the remote site which are either mounted on the robot or on the vehicle carrying the robot, to pick up various cues for the operator. For example, a video camera can be used to pick visual cues, a force and torque sensor mounted on the end-effector of the robot can provide force cues, and a microphone may be used to pick up audio cues from the remote site [19].

In bilateral force feedback tele-operation systems, the input device can vary in its technological complexity, ranging from a 6 degree of freedom position control device [20] to an exoskeletal arm [21] which is kinematically similar to the actual remote manipulator. Very often force display is provided through the controller or input device. The control input is sent to the remote manipulator which moves accordingly at the remote site. The movement of the manipulator and the status of remote environment are picked up by the sensors and displayed to the operator, thereby establishing a continuous closed loop control of the remote manipulator [22].

2.1.3. Control of End Effector

Tele-operation tasks require control of the end-effector of the remote manipulators, which have up to 6 degrees of freedom. Unlike industrial robots, which perform very similar routine manipulation tasks with low variability, tele-operation is suitable for performing tasks in environments which have low accessibility for human presence and high variability.

The tele-operation environment can change because of many reasons: the tele-operation site can change, the location of the objects in the environment might change from one instance to another even if tele-operation is performed on the same site, or the task changes from one instance to another. Since most tele-operation tasks have a high variability, it makes them unsuitable to be performed by completely automated systems, as is the case in industrial robotics. Tele-operation tasks need the additional capability of the human operator to understand and modify the task.

2.1.4. Degree of Certainty in the Remote Environment

Another characteristic of tele-operation tasks is the degree of certainty in the remote environment. It refers to the degree of certainty with which the task and its environment at the remote site are known at the local site. This characteristic implicates the extent to which remote task can be automated.

Tele-operations are used in place of robots when robots are unable to overcome either the evolutionary situation of a task performing or the demands in skillfulness of such a task. Therefore, they are kinds of robotic devices that combine human and

machine. Consequently, the man-machine link is of prime importance and provides the main difference with usual robot design.

2.2. Virtual Reality Based Tele-operation

First tele-operation systems were built after the Second World War for needs in nuclear activities [14]. They all used the master-slave concept. They are composed with two symmetrical arms. The master arm is handled by the operator; the slave one replicates the operator motions at the spot where the task has to be performed. In the earlier systems, master and slave were mechanically connected. Then, they were electrically powered giving the possibility of any distance between master and slave. In the 1980's, computers were introduced as control systems starting the way to Computer Aided Tele-operation. Nowadays, this Computer Aided Tele-operation utilization is greatly changed with the presence of Virtual Reality techniques.

In early systems, the absence of sophisticated electronics obliged to a symmetrical mechanical device to correctly transfer the motions from the operator to the slave device. Computer made possible a difference of shape in master and slave devices. When the slave kept its mechanical structure, the master could be reduced into a lot of different mini-systems easy to move by the operator. However these new interfaces better adapted to man did not reduce the general difficulty to correctly achieve the task. Additionally, in remote action, it is needed to have a good vision of what happens in the slave environment. Classic cameras, even stereoscopic, did not succeeded in adequately informing the operator who was very often disoriented, lost his subject of interest. Here also, VR techniques improve the situation, due to partial or total immersion opportunity.

Virtual reality is applied to tele-operation as assistance could improved the tele-operation efficiency both from ergonomic and friendly using point of view as well as from an information feedback point-of-view. Ideally, virtual reality using in tele-operation is expected to expand the application field to any task relevant to tele-work, whatever the dangerousness for man of any environment.

2.2.1 . Virtual Reality Background Information

Virtual reality is the use of various computer graphic systems in combination with various display and interface devices to provide the effect of immersion in an interactive three-dimensional computer-generated environment in which the virtual objects have spatial presence. This interactive three-dimensional computer-generated environment is called a virtual environment. By immersion it means the sense that either the user's point of view or the user's body is contained within the computer-generated space. By presence it means that the computer-generated objects in the virtual environment have an apparent position in the three-dimensional space relative to the user [23].

Virtual reality technique is applied in human in the-loop or human centered advanced simulation or prototyping systems. The most important feature of the concept is the multi-modality of the man-machine interaction, which involves all human sensory modalities. Among these capabilities, the haptic modality is of prime importance when human operator need to manipulate and touch virtual objects with realistic sensations of stiffness, roughness, temperature, shape, weight, contact forces, etc [2]. These physical parameters are collected then interpreted by the human haptic modality through a direct touch and motion of human body. Virtual environments are visually rendered to the

human operator through screens, head mounted displays and other up-to-date advanced visual interfaces. In the contrary to vision and auditory, haptic displays are active. To render and display forces, the interfaces must be able to both constraint human desired motions and, to apply forces on the involved human part. These interfaces are typically robotic devices that are capable to collect desired human motion or force to be sent to the virtual environment, and to display subsequent virtual forces calculated by computer algorithms to the human operator.

2.2.2. Shared Haptic Virtual Environment

Shared Haptic Virtual Environment can be grouped in three major classes: static, collaborative and cooperative shared virtual simulations [24].

- In a static virtual environment, each user can explore by looking and touching, but not modify the environment. Users may or may not see each other during the simulation, but cannot touch each other. Examples are browsing geometrical or shared databases on the net.
- In a collaborative virtual environment users can modify the environment but may not simultaneously shape or move the same virtual object. This scheme can be applied for surgical or professional training, co-located CAD and entertainment.
- In a cooperative virtual environment users can simultaneously modify the same virtual object. Users can see and touch each other, directly or indirectly through a common object. Possible applications are like those for collaborative environments.

2.2.3.The Static Shared Virtual Environment

After connecting to the server, the user locally replicates the virtual environment by either downloading the full Virtual Environment database or periodically requesting information pertinent to the immediate neighborhood. At the user level this is analogous to a single user simulation since there is no interaction with others. Therefore, any communication delay does not affect this scheme.

2.2.4. Collaborative Virtual Environment [25]

In a collaborative virtual environment only one user at a time can simultaneously edit the same virtual object. Replication of the VE at each user site is convenient to reduce delay in the haptic rendering loop. However, since these local copies can be modified during object manipulation, special care must be taken in enforcing a coherent representation of the virtual environment. There are two alternatives to synchronize users access to the virtual environment:

1) Central Server: a central server acts as a scheduler and keeps the only official copy of the virtual environment. Whenever a user gets close enough to an object, a request to edit is sent to the server. The server processes these requests in a first-come-first-serve basis, granting ownership and locking the object to prevent modification form other users. Other users are still allowed to touch and modify their own copy, however these changes will not be copied at the server site. After the user owning the object has finished editing and moves away, the object representation modified at the user site is sent and updated at the server site. A request to release object ownership is then sent to the server. The server

sends the new object representation to all other users and then assigns the object ownership to the next user. Client-Server connectivity fits well with this implementation.

2) Token Ring: users own the right to edit an object according to some predefined rules. In a token ring implementation users are sequentially given permission to edit. After the client owning permission to edit has completed the task, it sends a message to the next user passing ownership. There is no official copy of the VE at the server site, but this is passed around from user to user, instead. Since there is no need for a central server, Peer-to-Peer connectivity fits well with this implementation. Note that for Client-Server connectivity all communications are directed to-from a server. The server must process all incoming data, and then broadcast them. This scheme clearly does not scale well as the number of users increases since the server is over-loaded. In Peer-to-Peer connectivity the computational load is distributed more homogeneously in the system, and exchange of information is faster between different users since does not need to pass through the server. Multicasting can further reduce the communication load.

In both Central Server and Token Ring schemes, the haptic rendering loop is executed at each user site on a local replica of the virtual environment.

2.2.5. Dead Rechoning Techniques [26]

One example of utilizing this technique is the multi-player ball game. The system connectivity is Peer-to-Peer to reduce communication delay. All players send their relative position to the other players and the server periodically. These messages are also used to check heart beating, in other words, to check that all connections are still alive.

After hitting the ball, the active player broadcasts the new position and speed of the ball to the other players. Non-active players update the position of the ball on a local replica. Once a packet from the active player signals a collision, the new data is used to adjust the estimated position. Graphics and force rendering are synchronous with communication.

2.2.6. Cooperative Virtual Environment [25]

In a Haptically Cooperative Environment users can simultaneously manipulate and haptically feel the same object. This also involves the ability of feeling and pushing other users while moving in the simulation. The possibility of kinesthetically interacting with other users makes the simulation truly realistic. On the other hand, this also poses stringent constraints on the system layout and the maximum allowable communication latency. Haptically Cooperative Environments are potentially beneficial for:

1) Training of a team of professionals: force feedback has already been integrated into virtual surgical simulators. Let's imagine a team operating on the same real patient. Each team member interaction with the patient is perceived by all the other members, indirectly when pulling the patient tissue, or directly because of collisions in the limited workspace. These factors might need to be reproduced in a realistic simulation.

2) Entertainment: adding force feedback, thus allowing participants to kinesthetically interact with each other, adds a new dimension of fun.

3) Telerobotics: a telemanipulation system shares many aspects of a shared virtual environment [27]. In current implementations, the mix of virtual fixtures and real

manipulators enhance the quality and safety of the remote manipulation. Remote manipulation could be shared among multiple users.

Because multiple users are simultaneously interacting on the same object, it is necessary to allow only one dynamic engine to modify the object position, and only one shape modification engine to modify its shape. These are in fact the only two modules that change the status of the virtual environment. A possible solution is to perform all the computation at the server site, while the clients are simply sending to the server their haptic display (or pointing device) positions, and receiving the force-torque vectors to apply back to the users. This system architecture can be improved by distributing the collision detection engine among the clients. Each client performs its own collision detection, calculates its own interaction forces with the virtual environments, and then sends the information to the server that will update positions and shapes. The collision detection engine on the server site is responsible to calculate collisions between virtual objects.

The problem that allowing simultaneous manipulation is to enforce coherency. It is not possible to run the dynamic engine on a local replica of the virtual environment. This means that the local copy is updated with a certain delay after manipulation occurs, since data processing is performed at the server site. Kinesthetically linking remote users is therefore particularly challenging.

2.3. Force Feedback Devices and Its Application

Force feedback devices used for advanced haptic interaction include the PHANToM created by sensible Technologies [28], the FEELit mouse from Immersion Corporation and the Pantograph from Haptic Technologies [29]. Earlier graphical user interfaces (GUIs) provided tactile feedback through vibrations to the fingertips but they were unable to provide the more complex sensations of the force feedback devices.

Research in human haptics describes how the user experiences the sense of touch. The hand contains sensors or receptors that are in contact with the force feedback applied by the actuators, the kinesthetic and tactile information is sent to the brain which encodes it and sends motor commands to the muscles in response to the original force. The human and computer haptic systems work in a similar closed loop structure [30].

Research in haptic interface development increased with the need for improving hand-eye co-ordination on a conventional desktop. Using touch and force feedback was seen as a way of reducing the visual overload found on the increasingly complex desktop interfaces. The use of haptic devices was examined over a range of tasks including the Fitts tapping task, a searching and scrolling task and a steering-targeting task. The devices hoped to improve performance in relation to speed, a reduction in errors and in the workload of the user.

There are many applications that require feedback information to a human operator, tele-operation, tele-presence, virtual reality simulators such as virtual surgery training, driving simulators, etc. Commonly, haptic cues are fed back by using an

actuated mechatronic device able to constraint the operator desired motion against the applied reaction forces. Contrarily to the vision or auditory human modalities, haptic cues are collected through a bilateral coupling between the human held or worn haptic display and a remote robotic system. It is able to replicate human desired motions and to collect haptic information during contact or constraint motions.

Other applications based on virtual reality techniques, such as haptic feedback surgery training simulators, require also haptic devices to experience haptic interaction between the human operator and virtual environments. This is made by using computer haptic algorithms which compute collision detection and subsequent dynamic response motions and forces during contact with virtual objects. Consequently, haptic devices are commonly active actuated mechatronic devices which must be controlled stably to be correctly used and to avoid danger for operator.

In recent years, many researches have revealed that feeling objects in a shared virtual environment simultaneously can markedly enhance the effectiveness of many virtual reality applications [3]. Cooperative shared haptic virtual environments, where the users can simultaneously manipulate and haptically feel the same object, is potentially beneficial and in some cases could be indispensable. It could be useful for training as in, for example, virtual surgical simulators [3] where the team performs on the same real patient; all the other members perceive each team member interaction with the patient directly, when dealing with the patient's tissue, or indirectly because of the collisions in the limited workspace. However, the interaction feeling and its effect should be provided

to ensure that the perceptual experience in the virtual world corresponds to that in the real world, otherwise the training would be useless.

Another use of a haptic technology is in the entertainment industry, which would allow the participants to kinesthetically interact with each other. This adds a new dimension of enjoyment and brings the users one step closer to more realistic interactivity. Moreover, there will be a great benefit from such kinesthetic interaction in some sports training systems, especially the kind of multi-players sports that include direct contact between the players such as boxing, sumo wrestling, and football. The resulting virtual training system has the potential to be more realistic and efficient. In addition, there are many advantages of multi-hand manipulation that can be realized from daily life. More precise manipulation can be achieved using both hands. Also, the manipulation with both hands is more efficient than one hand as has been mentioned by some ergonomic studies [21]. Nevertheless, many virtual reality applications in architecture, industry, aerospace, automotive, entertainment, visualization, and education can be benefited from adding the sense of touch and making its sharable between distributed users. The haptic feedback improves the task performance in shared VE of participants as well as their sense of togetherness.

2.4. Instability Caused by Communication Delay

As discussed in Chapter 1, there are a number of issues related to bilateral tele-operation systems, namely transparency issues, communication bandwidth issues, continuous manual control issues, operation safety and error issues, autonomy issues and time delay issues. Among these, we are interested in the time delay issue.

In this section, we will analyze the stability issue caused by time delay for a linear system. Let us consider the following dynamical system

$$\begin{aligned} \dot{x}(t) &= Ax(t) + Bu(t-\tau), \qquad x(0) = x_0, \qquad u(0) = u_0 \\ y(t) &= Cx(t) \end{aligned} \tag{2.1}$$

where u is the control input, x is the state variable, y is the output, τ is the delay, and u_0 is the initial condition of the input, A, B, and C are constant matrices of appropriate dimensions for the process. It is assumed that (A, B) is a controllable pair and (C, A) is an observable pair. The transfer function of the closed loop system using static unit feedback relating the output, $y(t)$, to the desired input $y_d(t)$ (see Figure 2.1) is given by

$$\frac{Y(s)}{Y_d(s)} = \frac{C(sI-A)^{-1}Be^{-s\tau}}{1+C(sI-A)^{-1}Be^{-s\tau}} \tag{2.2}$$

where s is the Laplace transformation variable and $D(s)=e^{-\tau s}$, τ is time delay. $G(s)$ is the open loop transfer function of system illustrated in Figure 2.1.

In the above equation, the characteristic equation of the closed loop system contains the time delay element leading to an infinite number of eigenvalues. Controlling an infinite number of eigenvalues is not practically feasible. Furthermore, by a simple Taylor series expansion of $e^{-s\tau}$ one may generate poles in the right half plane so that the system is unstable.

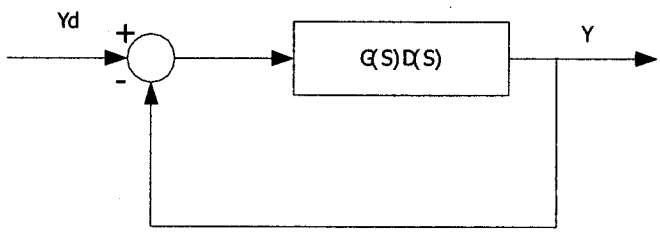

Figure 2.1. Linear System with Delay.

2.5. Current Work on Time Delay Issues

A lot of work has been done as to stabilize the tele-operation system with delay. Among them there are some successful solutions: scattering theory based controller design [31]; Smith-prediction based haptic feedback controller design [32]; and model based theory [33]. Below these solutions will be reviewed.

2.5.1. Scattering Theory Based Controller Design

A two-port network can be shown as in Figure 2.2, where F is the force applied across the system and V is the velocity injected into the system.

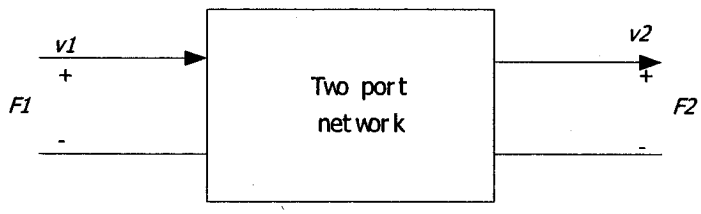

Figure 2.2. Two Port Network.

In Anderson and Spong's scattering theory [31], a scattering operator S is defined by

$$F - v = S(F + v) \tag{2.3}$$

which maps effort plus flow into effort minus flow, where the flow is entering the system's port and the effort is measured across the system's port.

As specified by Hannaford in [3], the relationship between effort F and flow v for a two-port network can be expressed as

$$\begin{bmatrix} F_1(s) \\ -v_2(s) \end{bmatrix} = \begin{bmatrix} h_{11}(s) & h_{21}(s) \\ h_{12}(s) & h_{22}(s) \end{bmatrix} \begin{bmatrix} v_1(s) \\ F_2(s) \end{bmatrix} = H(s) \begin{bmatrix} v_1(s) \\ F_2(s) \end{bmatrix} \tag{2.4}$$

In the case of a two-port network, this scattering matrix can be related to the hybrid matrix $H(s)$ as follows, where F_1, v_1 are the force and velocity for the left port, and F_2, v_2 for the right port,

$$\begin{bmatrix} F_1(s)-v_1(s) \\ F_2(s)+v_2(s) \end{bmatrix} = \begin{bmatrix} 1 & 0 \\ 0 & -1 \end{bmatrix} \left(\begin{bmatrix} F_1(s) \\ -v_2(s) \end{bmatrix} - \begin{bmatrix} v_1(s) \\ F_2(s) \end{bmatrix} \right)$$

$$= \begin{bmatrix} 1 & 0 \\ 0 & -1 \end{bmatrix} (H(s)-I) \begin{bmatrix} v_1(s) \\ F_2(s) \end{bmatrix} \tag{2.5}$$

In equation (2.5) a hybrid matrix $H(s)$ is defined.

Likewise,

$$\begin{bmatrix} F_1(s)+v_1(s) \\ F_2(s)-v_2(s) \end{bmatrix} = \begin{bmatrix} F_1(s) \\ -v_2(s) \end{bmatrix} + \begin{bmatrix} v_1(s) \\ F_2(s) \end{bmatrix}$$

$$= (H(s)+I) \begin{bmatrix} v_1(s) \\ F_2(s) \end{bmatrix} \tag{2.6}$$

Therefore, from equations (2.3), (2.5), and (2.6), one gets

$$\mathrm{S(s)} = \begin{pmatrix} 1 & 0 \\ 0 & -1 \end{pmatrix} (H(s)-I)(H(s)+I)^{-1} \tag{2.7}$$

where S(s) is the scattering operator for the two-port network.

According to scattering theory, a system is passive if and only if the norm of its scattering operator is less than or equal to one, which can be shown based on passivity theory [31].

Now let us see the effects of time delay on the stability of the system by using scattering theory. A bilateral tele-operation system with communication delay can be shown as in Figure 2.3. The communication block in Figure 2.3 can be expressed as in equation (2.8), where T is the time delay due to telecommunication, F_{md} is the feedback force for the master side after time delay, F_s is the force feedback from the slave side, v_{sd} is the injected velocity for slave side after the time delay, and v_m is the velocity injected from master side.

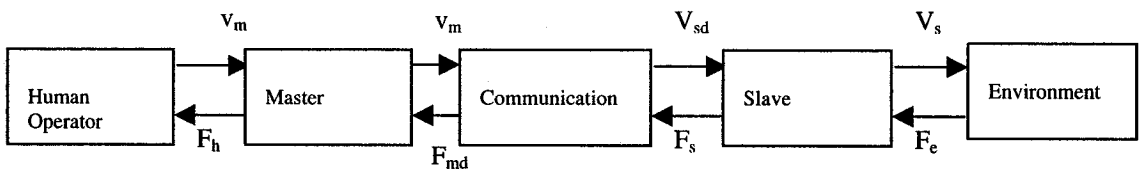

Figure 2.3. Bilateral tele-operation system with communication delay.

$$\begin{aligned} F_{md}(t) &= F_s(t-T), \\ v_{sd}(t) &= v_m(t-T) \end{aligned} \tag{2.8}$$

The associated hybrid matrix is derived directly as

$$H(s) = \begin{bmatrix} 0 & e^{-sT} \\ -e^{-sT} & 0 \end{bmatrix} \tag{2.9}$$

using equation (2.7), we can calculate the scattering matrix for the system.

$$
\begin{aligned}
S &= \begin{bmatrix} 1 & 0 \\ 0 & -1 \end{bmatrix} (H(s) - I)(I + H(s)^{-1}) \\
&= \begin{bmatrix} 1 & 0 \\ 0 & -1 \end{bmatrix} \begin{bmatrix} -1 & e^{-sT} \\ -e^{-sT} & -1 \end{bmatrix} \begin{bmatrix} 1 & e^{-sT} \\ -e^{-sT} & -1 \end{bmatrix}^{-1} \\
&= \begin{bmatrix} -\tanh(sT) & \operatorname{sech}(sT) \\ \operatorname{sech}(sT) & \tanh(sT) \end{bmatrix}
\end{aligned}
\tag{2.10}
$$

The L_2 norm of S is given by

$$
\begin{aligned}
\|S\| &= \sup_{\omega} \lambda^{1/2} \left(\begin{bmatrix} j\tan(\omega T) & \sec(\omega T) \\ \sec(\omega T) & -j\tan(\omega T) \end{bmatrix} \begin{bmatrix} -j\tan(\omega T) & \sec(\omega T) \\ \sec(\omega T) & j\tan(\omega T) \end{bmatrix} \right) \\
&= \sup_{\omega} \lambda^{1/2} \begin{bmatrix} \tan^2(\omega T) + \sec^2(\omega T) & 2j\tan(\omega T)\sec(\omega T) \\ -2j\tan(\omega T)\sec(\omega T) & \tan^2(\omega T) + \sec^2(\omega T) \end{bmatrix}
\end{aligned}
\tag{2.11}
$$

where $\lambda^{1/2}(\cdot)$ denotes the square root of the maximum eigenvalue, so that

$$
\|S\| = \sup_{\omega} (|\tan(\omega T)| + |\sec(\omega T)|) = \infty
$$

Therefore, the scattering operator for the time delay system is unbounded and hence the system is not passive, in other words, the time delay destabilizes the system [31].

Based on the definition of scattering operator as in this section, and the conditions for passivity, the controller can be designed for system with time delay. The basic idea is to choose the control law so that the two-port characteristics of the communication block are identical to a two port lossless transmission line.

A linear two-port lossless transmission line element having an input/output relationship in the frequency domain as described in reference [31] can be expressed as:

$$\begin{aligned} F_1(s) &= Z_0 \tanh(sl/v_0)v_1(s) + \sec h(sl/v_0)F_2(s) \\ -v_2(s) &= -\sec h(sl/v_0)v_1(s) + (\tanh(sl/v_0)/Z_0)F_2(s) \end{aligned} \tag{2.12}$$

where $Z_0 = \sqrt{l/c}$, $v_0 = 1/\sqrt{lc}$, l is the characteristic inductance, and c is the capacitance for the transmission line.

In equation (2.12), set Z_0=1 and v_0=l/T, which gives:

$$\begin{aligned} F_{md}(s) &= \tanh(sT)v_m(s) + \sec h(sT)F_s(s) \\ -v_{sd}(s) &= -\sec h(sT)v_m(s) + \tanh(sT)F_s(s) \end{aligned} \tag{2.13}$$

The tele-operation system with time delay can now be represented as:

$$\begin{bmatrix} F_{md}(s) - v_m(s) \\ F_s(s) + v_{sd(s)} \end{bmatrix} = \begin{bmatrix} 0 & e^{-sT} \\ e^{-sT} & 0 \end{bmatrix} \begin{bmatrix} F_{md}(s) + v_m(s) \\ F_s(s) + v_{sd}(s) \end{bmatrix} \tag{2.14}$$

thus the scattering matrix for the communication block S is given by

$$\mathrm{S} = \begin{bmatrix} 0 & e^{-sT} \\ e^{-sT} & 0 \end{bmatrix} \tag{2.15}$$

The norm of the scattering matrix is given by

$$\|S\| = \sup_w \lambda^{1/2}(S^*(jw)S(jw)) = \sup_w \lambda^{1/2}\left(\begin{bmatrix} 1 & 0 \\ 0 & 1 \end{bmatrix}\right) = 1 \tag{2.16}$$

In time domain, the control law presents in equation (2.14) can now be derived as [31]

$$F_{md}(t) = F_s(t-T) - v_{sc}(t-T) + v_{m(t)}$$

$$v_{sd}(t) = v_m(t-T) - F_s(t) + F_{md}(t-T) \tag{2.17}$$

Because the force and the velocity signals may differ by orders of magnitude, the control law given in equation (2.17) may have implementation problems. In order to overcome this, a scaling factors n is added and the control law becomes:

$$F_{md}(t) = F_s(t-T) + n^2(v_m(t) - v_{sd}(t-T))$$

$$v_{sd}(t) = v_m(t-T) + \frac{1}{n^2}(F_{md}(t-T) - F_s(t)) \tag{2.18}$$

By applying the above control law, the communication block mimics a lossless transmission line and is therefore guaranteed to be a passive element independent of the time delay. Thus the overall system is guaranteed to be stable [31].

2.5.2. Smith-Predictor Based Haptic Feedback Controller Design

Adams et. al. [34] presented an approach using the so called "virtual coupling" network between the haptic device and the held virtual object. The virtual coupling allows the environment design to be separated from the sampled-data control issues associated with the haptic display. The main advantage of such a control design is that the parameterization of the virtual mechanism used as a coupling between the haptic

interface and the manipulated virtual object can be elaborated so that the passivity of the whole system is preserved using linear interconnected network theory.

A one degree-of-freedom haptic display can be shown as in Figure 2.4, where *M* is the transfer function of the haptic device, *E* is the transfer function of the virtual environment, and C is the virtual coupling.

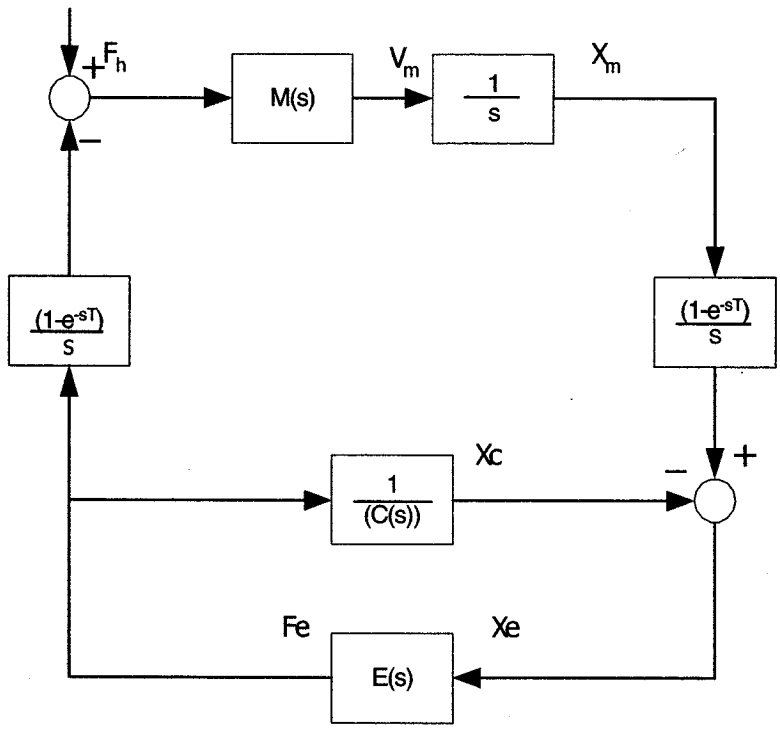

Figure 2.4. Model of one DOF haptic display.

The control scheme of the haptic interaction will contain a time delay between the virtual coupling and the virtual environment in both directions as presented in Figure 2.3

by the communication channel. In the continuous time case, the transfer function from F_h to F_e is given by

$$\left[(F_h - F_e e^{-s\tau_2})\frac{M(s)}{s} - F_e e^{-s\tau_2} C(s)\right] e^{-s\tau_1} E(s) = F_e \tag{2.18}$$

We have $$\frac{F_e(s)}{F_h(s)} = \frac{(1/s)M(s)E(s)e^{-s\tau_1}}{1 + e^{-s(\tau_1+\tau_2)}E(s)((1/s)M(s) + C(s))} \tag{2.19}$$

It follows clearly that the obtained closed loop system has infinite eigenvalues because the time delay element is present in the characteristic equation which does imply the potential instability of the closed loop system.

By utilizing a simple Smith predictor based controller as obtained in Figure 2.5 to system as shown in Figure 2.4, the resulting transfer function of the closed loop system is a stable haptic simulation with a delayed input as given below

$$\frac{F_e(s)}{F_h(s)} = \frac{(1/s)M(s)E(s)e^{-s\tau_1}}{1 + E(s)((1/s)M(s) + C(s))} \tag{2.20}$$

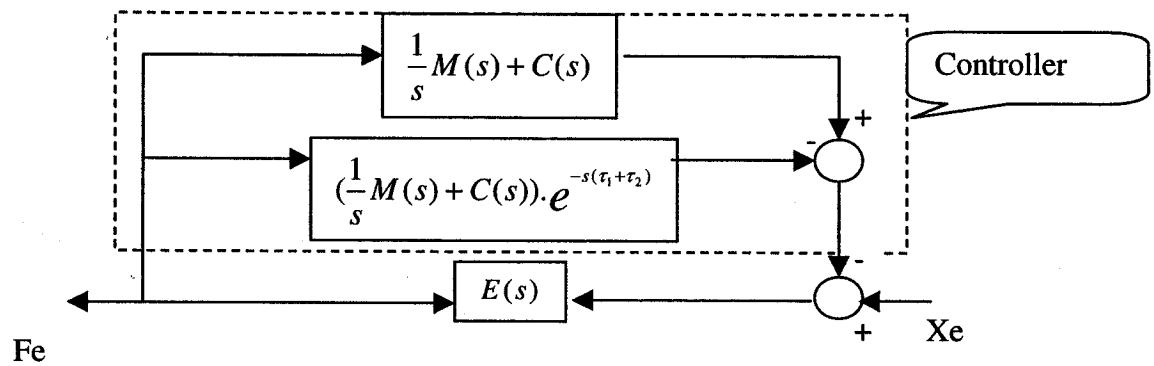

Figure 2.5. Smith predictor based controller.

The purpose of the controller based on the Smith prediction principle is to eliminate the delayed response F_e from the master part and replace it with a non-delayed response. The resulting closed loop system is a system in which the delay is only in the force applied by the operator.

2.5.3. Model Based Theory

Arioui and Mammar [35] have done a lot of work in the model based controller design for the time-delayed tele-operation systems. Model of the interconnected systems with time delay can be depicted as in Figure 2.6. where, G_1 and G_2 are the time domain mapping of two interconnected systems, e_1 and e_2 are external input signals of the interconnected systems, and u_1 and u_2 are the controller's signal. The output singnals y_1 and y_2 are delayed by time delay T_1 and T_2.

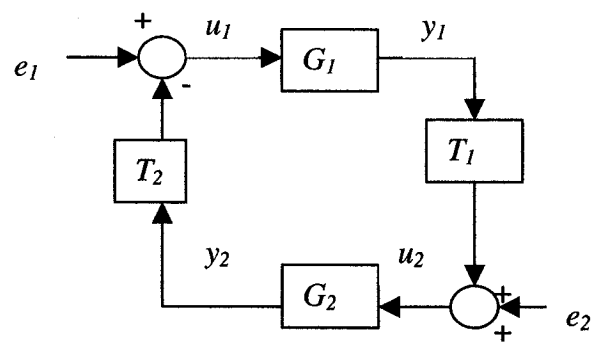

Figure 2.6. Model of the interconnected systems with time delay.

A simple model based controller to stablize the inter-connected system is depicted as in Figure 2.7, where u_1, u_2, y_1, y_2, G_1, G_2, T_1, T_2 have the same definition as in Figure 2.7, and $y_{11} = G_1(y_2(t-T_2))$ and $y_{12} = G_1(y_2(t))$.

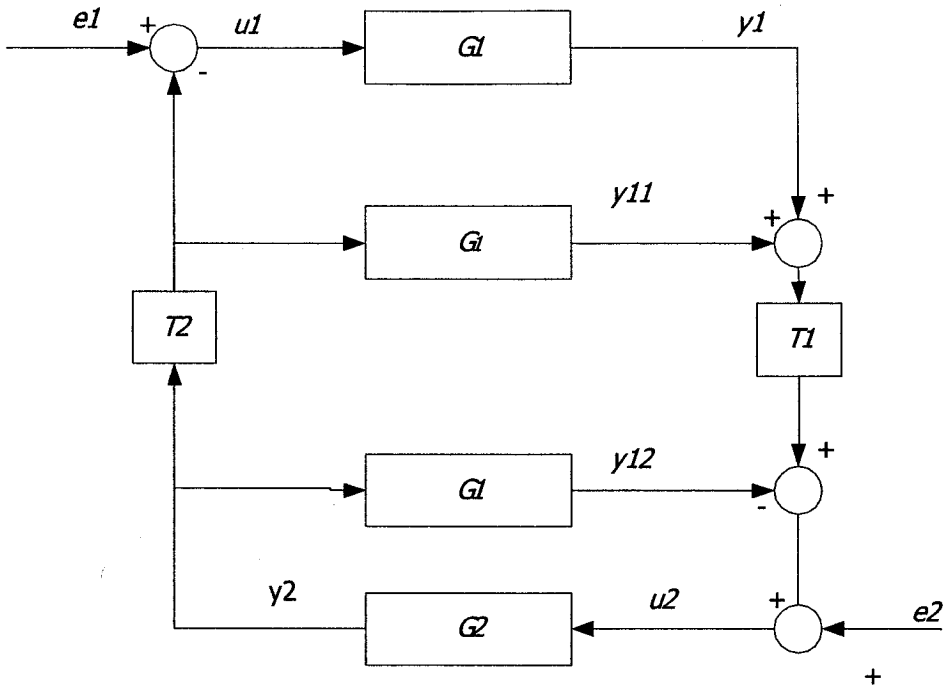

Figure 2.7. Model based controller.

From Figure 2.7, we obtain:

$$\begin{cases} u_1(t) = e_1(t) - y_2(t - T_2(t)) \\ u_2(t) = e_2(t) + y_1(t - T_1(t)) + y_{11}(t - T_1(t)) - y_{12}(t) \end{cases} \tag{2.11}$$

The second equation can be re-written in the following form:

$$u_2(t) = e_2(t) + G_1(e_1(t - T_1(t)) - y_2(t)) \tag{2.12}$$

As shown in [35], when $T_1 = T_2 = 0$, if G_1 and G_2 are passive then the resulting interconnected system with inputs (e_1, e_2) and output (y_1, y_2) is also passive. Equation (2.12) shows that the final resulting system is equivalent to the system of Figure 2.6 with $T_1 = T_2 = 0$, but with a delayed input $e_1(t - T_1(t))$. The passivity of the overall system

holds since there is no hypothesis made on e_1 and e_2, and the passivity property was shown whatever e_1 and e_2 are [35].

2.6. Conclusion

In this chapter, we presented some background information about tele-operation technology. Tele-operation is suitable for performing tasks in environments which have low accessibility for human presence and high variability. It has already been applied to oil industry, undersea operation, aerospace industry and so on. With the help of virtual reality, tele-operation could be and has been used on medical training (surgery), tele-operation in all kinds of remote environment. How to transparently reflect the remote haptic or vision information to the operation is a key topic in this area, which involved a lot of research work in computer science and telecommunication domain. Researches have proved that haptic feedback is one of the most helpful information for the operators in local site to control the remote site. As a result, stability issue will be especially important, since unstable feedback signal will harm the operators. Time delay is the main factor that causes the instability of the system, and this thesis will mainly focus on this issue.

In this chapter, some solutions to the time delay issue have been introduced briefly. However, theses solutions have limitations. Scattering theory based method is based on the passivity theory, the controller designed can not perform well when the transmission delay is time varying; the smith prediction method is only good for linear system, and model based control requires the precise modeling of the system model. How to retain stability of the tele-operation system with time varying delay, and at the same

time ensure that the slave side operator movement precisely track that of the master side is the objective that we want to achieve in this thesis. In the following chapters, we will present our solution.

Chapter 3

Mathematical Model of Phantom Haptic Device

Different type of haptic devices have been developed in order to fulfill the bilateral tele-operation, and phantom haptic device from Sensable company is one of them. In this chapter we will investigate the mathematical system model based on the non linear model provided by [36] and [37]. In section 3.1 haptic display and haptic device is introduced in general purpose. In section 3.2 the phantom haptic device model is

investigated, and in section 3.3 this model is linearized and a state feedback controller is designed to stabilize the system around the operation point. In section 3.4, model validation is performed by applying the controller designed for the linear system to the nonlinear model, and comparing the control results by simulations.

3.1. Introduction to Haptic Display and Haptic Device

Haptic is a relatively recent enhancement to virtual environments allowing users to touch and feel the simulated objects they interact with. Current commercial products allow tactile feedback through desktop interfaces (such as the FEELIt mouse or the PHANToM arm)[2] and dextrous tactile and force feedback at the fingertips through haptic gloves (such as the CyberTouch and the CyberGrasp) [28].

3.1.1. Haptic Display

Haptic display refers to the mechanical device conFigured to convey kinesthetic cues to a human operator. Haptic displays vary greatly in kinematic structure, workspace, and force output. They can be broadly classified into two categories, those which "measure motion and display force" and those which "measure force and display motion" [5]. The former will be referred to as impedance displays, the latter as admittance displays. Impedance displays typically have low inertia and are highly back-drivable. The well known Phantom family of haptic displays, the McGill University Pantograph [23], and the University of Washington Pen-Based Force Display [23] fall into this class, along with many others. Admittance displays are often high-inertia, non back-drivable manipulators fitted with force sensors and driven by a position or velocity control loop.

Carnegie Mellon University's WYSIWYF Display, which is based upon PUMA 560 industrial robots, is a good example [23].

3.1.2. Haptic Interface

Haptic interface includes everything that comes between the human operator and the virtual environment. This always includes the haptic device, control software, and analog-to-digital/digital-to-analog conversion. It may also include a virtual coupling network which links the haptic display to the virtual world. The haptic interface characterizes the exchange of energy between the operator and the virtual world and thus is important for both stability and performance analysis. Virtual environment computer generated model of some physically motivated scene. The virtual world may be as elaborate as a high-fidelity walkthrough simulation of a new aircraft design, or as simple as a computer air hockey game. Regardless of its complexity, there are two fundamentally different ways in which a physically based model can interact with the haptic interface. The environment can act as an impedance, accepting velocities (or positions) and generating forces according to some physical model. The other possibility is for the virtual environment to act as an admittance, accepting forces and returning velocities (or positions) [5].

3.1.3. Haptic Simulation

Haptic simulation synthesizes human operator, haptic interface, and virtual environment which creates a kinesthetically immersive experience. All of these elements are important in determining the stability of the system. The simulation includes

continuous components, such as mechanical device, as well as digital components, like the virtual world model and control software.

The structure of the haptic system has four possibilities corresponding to the choice of haptic display type (impedance or admittance) and virtual environment type (impedance or admittance). Previous work has almost always focused on one of these four combinations, making results specific to that particular case.

3.1.4. Phantom Haptic Device

Although many devices as mentioned above have been used as desktop interfaces, the PHANToM with 3-D force feedback information has been the preferred device of many of the experimenters for assessing the implications of haptic devices on human performance. The device is in the form of a stylus that can be moved on an x, y and z axis and a button is used in a similar way to a mouse button, for activating or picking up a target. The PHANToM is also available in the form of a thimble that allows the user to insert their finger and feel, touch and manipulate virtual objects. It appears as a mouse on the desktop in the form of a cursor. Optical sensors monitor changes in motion and movement of the stylus, this is sent to the computer, which in turn sends commands to mechanical actuators that provide the force feedback to the stylus or thimble. Information for this force feedback is provided in algorithms in the software for the virtual objects and desktop virtual environment [36].

A picture of the phantom haptic device is given as in Figure 3.1.

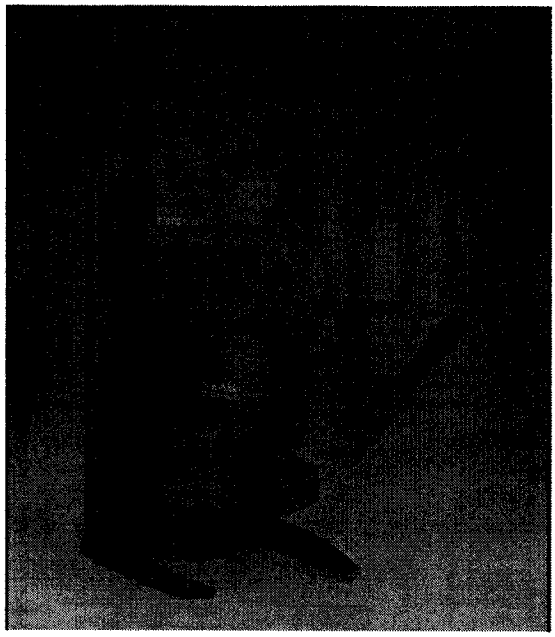

Figure 3.1. Photo of Phantom ™ Device [28].

The property of Phantom device can be summarized as follows [28]

Range of motion: Hand movement pivoting at wrist;
Nominal position resolution > 1100 dpi~ 0.023 mm;
Backdrive friction < 0.23 oz (0.06 N) ;
Maximum exertable force at nominal(orthogonal arms) position: 1.8 lbf. (7.9 N);
Continuous exertable force: 0.4 lbf. (1.75 N);
Stiffness X axis > 10.8 lb/in (1.86 N/mm), Y axis > 13.6 lb/in (2.35 N/mm),
Z axis > 8.6 lb/in (1.48 N/mm);
Inertia (apparent mass at tip) : ~0.101 lbm. (45 g) ;

Force feedback: x, y, z ;
Position sensing [Stylus gimbal]: x, y, z (digital encoders);
Interface Parallel port: IEEE-1394 FireWire® port;
Supported platforms Intel-based PCs;

3.2. Mathematical Model of Phantom Haptic Device

Since phantom haptic device has been applied on many haptic related researches, to get a precise model of it is very important. In [36] Murat Cenk Cavusoglu et al. have done a lot of work on the modeling of Phantom model 1.5 system. In this thesis, the mathematical model of the phantom device is based on the nonlinear model obtained by Murat et al [36], [37].

The nonlinear mathematical model of the phantom device may be expanded as:

$$\begin{bmatrix} M_{11} & 0 & 0 \\ 0 & M_{22} & M_{23} \\ 0 & M_{32} & M_{33} \end{bmatrix} \begin{bmatrix} \ddot{\theta}_1 \\ \ddot{\theta}_2 \\ \ddot{\theta}_3 \end{bmatrix} + \begin{bmatrix} C_{11} & C_{12} & C_{13} \\ C_{21} & 0 & C_{23} \\ C_{31} & C_{32} & 0 \end{bmatrix} \begin{bmatrix} \dot{\theta}_1 \\ \dot{\theta}_2 \\ \dot{\theta}_3 \end{bmatrix} + \begin{bmatrix} 0 \\ N_2 \\ N_3 \end{bmatrix} = \begin{bmatrix} \tau_1 \\ \tau_2 \\ \tau_3 \end{bmatrix} \tag{3.1}$$

Where M_{11}, M_{22}, M_{23}, M_{32}, M_{33}, C_{11}, C_{12}, C_{13}, C_{21}, C_{23}, C_{31}, C_{32}, N_2, and N_3 are defined as in Appendix 1.

The states of the haptic system are therefore selected as:

$$x_1 = \theta_1,\ x_2 = \dot{\theta}_1,\ x_3 = \theta_2,\ x_4 = \dot{\theta}_2,\ x_5 = \theta_3,\ x_6 = \dot{\theta}_3.$$

The relationship between force input and velocity output can be illustrated as in Figure 3.2, and the Jacobian of the manipulator is given by [36]

$$J(\theta)=\begin{bmatrix} l_1 & -l_1\sin(\theta_1)\sin(\theta_2) & \sin(\theta_1)(l_2+l_1\sin(\theta_2)) \\ 0 & l_1\cos(\theta_2) & l_1(\cos(\theta_1)-\cos(\theta_2)) \\ 0 & -l_1\cos(\theta_1)\sin(\theta_2) & \cos(\theta_1)(l_2+l_1\sin(\theta_2)) \\ 0 & 0 & -\cos(\theta_1) \\ 1 & 0 & 0 \\ 0 & 0 & \sin(\theta_1) \end{bmatrix} \tag{3.2}$$

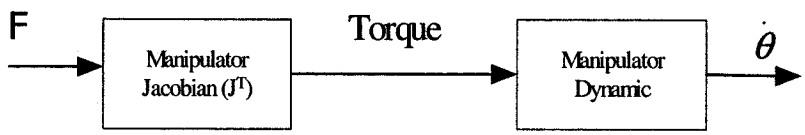

Figure 3.2 Relationship between force input and velocity output.

The torque τ applied to the manipulator is given by

$\tau = J^T(\theta)F$, where force $F = [f_x \quad f_y \quad f_z \quad 0 \quad 0 \quad 0]$, and f_x, f_y, and f_z are forces in x, y, and z axis.

The force and torque relationship now becomes

$$\begin{aligned} \tau_x &= 0.2150 f_x \\ \tau_y &= -0.2150\sin(x_1)\sin(x_3)f_x - 0.1700\cos(x_x)f_y - 0.2150\cos(x_1)\sin(x_3)f_z \\ \tau_z &= \sin(x_1)(0.1700+0.2150\sin(x_3))f_x + (0.2150\cos(x_1)-0.2150\cos(x_3))f_y \\ &\quad + \cos(x_1)(0.1700+0.2150\sin(x_3))f_z \end{aligned} \tag{3.3}$$

3.3. Phantom System Linearization

This thesis is concerned with design of a control scheme for the bilateral tele-operation system, where Phantom system is used as the haptic device in the tele-opeation system. The control of the phantom system is not the major issue for this thesis, but we need a stable device when we apply our control scheme.

In order to control the nonlinear system, we linearize the system at work point [0 0 0 0 0 0] and design a controller in linear system domain and apply this to the non linear system around the work point. The state space representation of the nonlinear haptic system is:

$\dot{X} = f(X,U)$, where $U = [f_x \quad f_y \quad f_z]$.

By linearizing the system at X=0, we have:

$$\dot{X} = \frac{\partial f}{\partial X}\Big|_{X=0,U=0} X + \frac{\partial f}{\partial u}\Big|_{X=0,U=0} U \tag{3.4}$$

The linearized system is given by:

$$\begin{aligned} \dot{X} &= AX + BU \\ Y &= CX + DU \end{aligned} \tag{3.5}$$

where A, B, C, and D are the matrices in state space, and are calculated as follows:

$$A=\begin{bmatrix} 0 & 1 & 0 & 0 & 0 & 0 \\ 0 & 0 & 0 & 0 & 0 & 0 \\ 0 & 0 & 0 & 1 & 0 & 0 \\ 0 & 0 & 0 & 0 & 0 & 0 \\ 0 & 0 & 0 & 0 & 0 & 1 \\ 0 & 0 & 2.2338 & 0 & 51.6471 & 0 \end{bmatrix}$$

$$B=\begin{bmatrix} 0 & 0 & 0 \\ 60.1600 & 0 & 0 \\ 0 & 0 & 0 \\ 0 & -70.0700 & 0 \\ 0 & 0 & 0 \\ 0 & 0 & 124.1000 \end{bmatrix}$$

$$C=\begin{bmatrix} 0 & 1 & 0 & 0 & 0 & 0 \\ 0 & 0 & 0 & 1 & 0 & 0 \\ 0 & 0 & 0 & 0 & 0 & 1 \end{bmatrix}$$

$$D=\begin{bmatrix} 0 & 0 & 0 \\ 0 & 0 & 0 \\ 0 & 0 & 0 \end{bmatrix}$$

With further calculations we can see the whole system is now decomposed into the following three subsystems, where y_1, y_2, and y_3 are the outputs of the subsystem.

Subsys1: $y_1 = G_{11} = \frac{60.16}{s} f_x$ (3.6)

Subsys2: $y_2 = G_{22} = \frac{-70.07}{s} f_y$ (3.7)

Subsys3:

$$y_3 = G_{23} f_y + G_{33} f_z = \frac{-156.5}{s^3 - 1.776e^{-15} s^2 - 51.65s} f_y + \frac{124.1s - 3.478e^{-9}}{s^2 - 1.776e^{-15} s - 51.65} f_z \qquad (3.8)$$

The transfer function block diagram of the linearized system is depicted in Figure 3.3

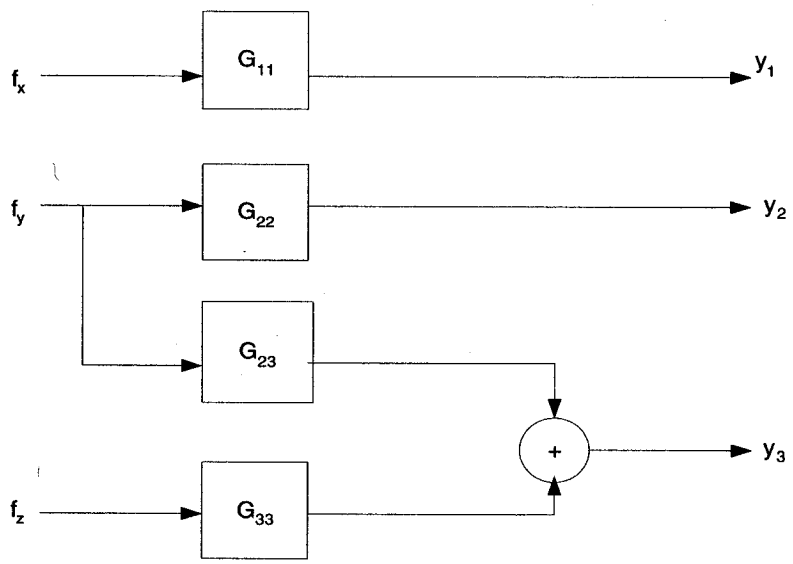

Figure 3.3. Block diagram of the linearized phantom haptic system.

We next design a state feed back controller to satisfy the following specifications:

(i) The settling time is less than 1s, and

(ii) The closed-loop poles of the system are placed at:

(-5+j, -5-j, -50+j, -50-j, -52+j, -52-j).

Consequently, the controller is obtained as:

$$K = \begin{bmatrix} 4.0685 & 0.8969 & 0 & 0 & -126.5335 & -2.4816 \\ 0 & 0 & -38.3043 & -1.4842 & 0 & 0 \\ -0.0096 & -0.0024 & 0.0181 & 0 & 2.8569 & 0.4517 \end{bmatrix}$$

After applying the controller to the linearized system, the closed loop system transfer function becomes:

$$\begin{bmatrix} y_1 \\ y_2 \\ y_3 \end{bmatrix} = \begin{bmatrix} T_{11} & T_{12} & T_{13} \\ T_{21} & T_{22} & T_{23} \\ T_{31} & T_{32} & T_{33} \end{bmatrix} \begin{bmatrix} f_x \\ f_y \\ f_z \end{bmatrix},$$

where elements in matrix T are given as:

$$T_{11} = \frac{60.16s^5 + 9692s^4 + 5.317\times10^5 s^3 + 1.102\times10^7 s^2 + 4.929\times10^7 s - 1.875\times10^{-7}}{s^6 + 214s^5 + 1.767\times10^4 + 6.92\times10^5 s^3 + 1.248\times10^7 s^2 + 8.145\times10^7 s + 1.759\times10^8}$$

$$T_{21} = \frac{7.159\times10^{-10} s^4 + 7.582\times10^{-8} s^3 + 2.216\times10^{-7} s^2 + 1.07\times10^{-5} s + 9.68\times10^{-11}}{s^6 + 214s^5 + 1.767\times10^4 + 6.92\times10^5 s^3 + 1.248\times10^7 s^2 + 8.145\times10^7 s + 1.759\times10^8}$$

$$T_{31} = \frac{17.95s^4 + 1983s^3 + 5.603\times10^4 s^2 + 1.947\times10^5 s - 1.337\times10^{-9}}{s^6 + 214s^5 + 1.767\times10^4 + 6.92\times10^5 s^3 + 1.248\times10^7 s^2 + 8.145\times10^7 s + 1.759\times10^8}$$

$$T_{12} = \frac{-8.795\times10^{-9} s^4 - 1.27\times10^6 s^3 - 6.107\times10^{-5} s^2 - 0.000979s - 7.209\times10^{-19}}{s^6 + 214s^5 + 1.767\times10^4 + 6.92\times10^5 s^3 + 1.248\times10^7 s^2 + 8.145\times10^7 s + 1.759\times10^8}$$

$$T_{22} = \frac{-70.07s^5 - 7708s^4 - 2.471\times10^5 s^3 - 1.935\times10^6 s^2 - 4.556\times10^6 s - 9.631\times10^{-20}}{s^6 + 214s^5 + 1.767\times10^4 + 6.92\times10^5 s^3 + 1.248\times10^7 s^2 + 8.145\times10^7 s + 1.759\times10^8}$$

$$T_{23} = \frac{-2.129\times10^{-9} s^4 - 2.278\times10^{-7} s^3 - 6.621\times10^{-6} s^2 - 2.756\times10^{-5} s - 4.188\times10^{-21}}{s^6 + 214s^5 + 1.767\times10^4 + 6.92\times10^5 s^3 + 1.248\times10^7 s^2 + 8.145\times10^7 s + 1.759\times10^8}$$

$$T_{31} = \frac{1.853\times10^4 s^4 + 2.872\times10^6 s^3 + 1.484\times10^8 s^2 + 2.555\times10^9 s + 3.215\times10^{-7}}{s^6 + 214s^5 + 1.767\times10^4 + 6.92\times10^5 s^3 + 1.248\times10^7 s^2 + 8.145\times10^7 s + 1.759\times10^8}$$

$$T_{32} = \frac{7.818\times10^{-9} s^4 + 1.038\times10^{-6} s^3 + 4.514\times10^{-5} s^2 + 6.395\times10^{-4} s + 5.832\times10^{-9}}{s^6 + 214s^5 + 1.767\times10^4 + 6.92\times10^5 s^3 + 1.248\times10^7 s^2 + 8.145\times10^7 s + 1.759\times10^8}$$

$$T_{33} = \frac{124.1s^5 + 1.96\times10^4 s^4 + 1.062\times10^6 s^3 + 2.127\times10^7 s^2 + 8.216\times10^7 s - 2.422\times10^{-7}}{s^6 + 214s^5 + 1.767\times10^4 + 6.92\times10^5 s^3 + 1.248\times10^7 s^2 + 8.145\times10^7 s + 1.759\times10^8}$$

By applying the controller and defining the state space representation of the closed loop system, we get

$$\dot{X}_c = A_c X + B_c F$$

$$Y_c = C_c X + D_c F$$

where

$$A_c = 1\times10^3 \times \begin{bmatrix} 0.001 & 0 & 0 & 0 & 0 & 0 \\ -0.2448 & -0.0539 & 0 & 0 & 7.6123 & 0.1493 \\ 0 & 0 & 0 & 0.001 & 0 & 0 \\ 0 & 0 & -2.7050 & -0.1040 & 0 & 0 \\ 0 & 0 & 0 & 0 & 0 & 0.001 \\ 0.0012 & 0.003 & 0 & 0 & -0.3029 & -0.0561 \end{bmatrix}$$

$$B_c = \begin{bmatrix} 0 & 0 & 0 \\ 60.16 & 0 & 0 \\ 0 & 0 & 0 \\ 0 & -70.07 & 0 \\ 0 & 0 & 0 \\ 0 & 0 & 124.10 \end{bmatrix}$$

$$C_c = \begin{bmatrix} 0 & 1 & 0 & 0 & 0 & 0 \\ 0 & 0 & 0 & 1 & 0 & 0 \\ 0 & 0 & 0 & 0 & 0 & 1 \end{bmatrix}$$

$$D_c = \begin{bmatrix} 0 & 0 & 0 \\ 0 & 0 & 0 \\ 0 & 0 & 0 \end{bmatrix}$$

3.4. Model Validation

In this section, model validation will be performed by applying the designed controller for linearized system to the nonlinear system. The simulations are performed at different initial conditions to verify if the controller designed for the linearized system works well or not for the nonlinear system.

Applying the controller to the linearized system zero input response of the system is shown in Figure 3.4 to Figure 3.9 with the following initial conditions:

$$X_{01} = [0.1 \quad 0 \quad 0.1 \quad 0 \quad 0 \quad 0]$$

$$X_{02} = [0.1 \quad 0 \quad 0 \quad 0 \quad 0.1 \quad 0]$$

$$X_{03} = [0 \quad 0 \quad 0.1 \quad 0 \quad 0.1 \quad 0]$$

$$X_{04} = \left[\frac{\pi}{2} \quad 0 \quad 0 \quad 0 \quad 0 \quad 0\right]$$

$$X_{05} = \left[0 \quad 0 \quad \frac{\pi}{2} \quad 0 \quad 0 \quad 0\right]$$

$$X_{06} = \left[0 \quad 0 \quad 0 \quad 0 \quad \frac{\pi}{2} \quad 0\right]$$

From the simulation results as shown in Figure 3.4 to Figure 3.9, we can see that the state feedback controller designed for the linearized system works well when the angle is at ththee maximum value which is $\pi/2$, so we can say the controller is applicable for the system at any initial value.

Figures 3.10 to 3.15 show the simulation results when we apply the designed state feedback controller to the nonlinear system. From these simulations we can find that the controller designed for the linearized system works well for the original nonlinear system inside the work space.

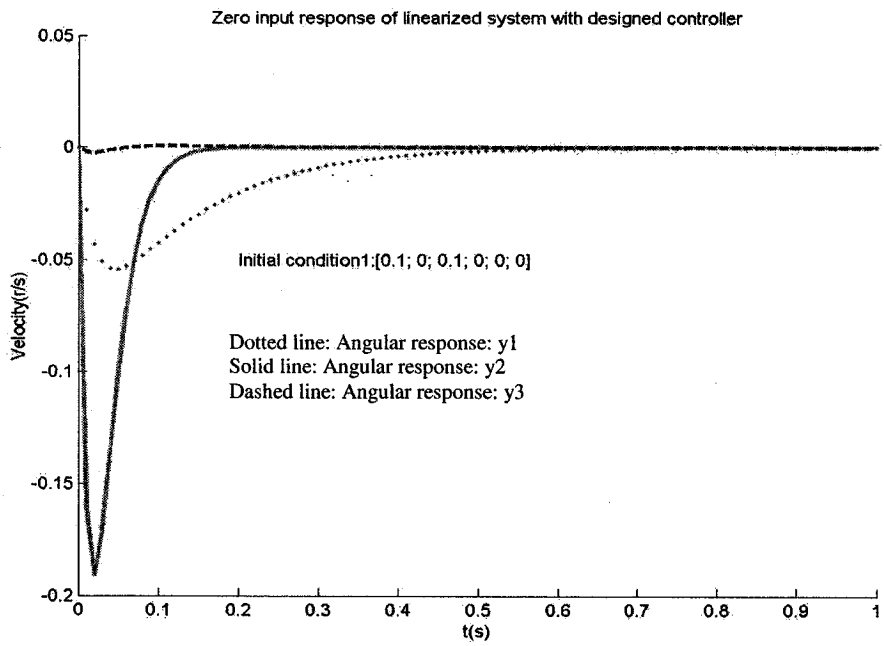

Figure 3.4. Zero input response of linearized system with initial condition 1.

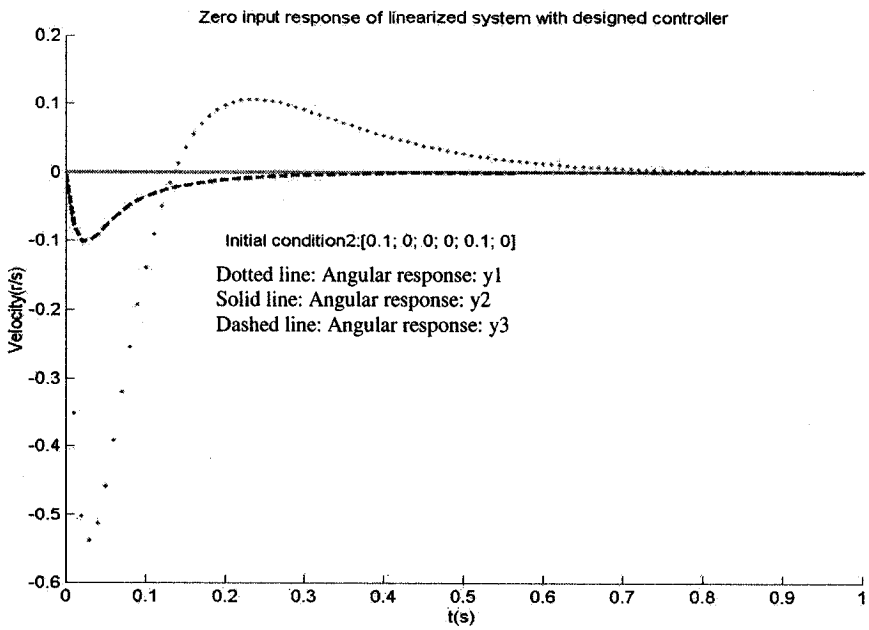

Figure 3.5. Zero input response of linearized system with initial condition 2.

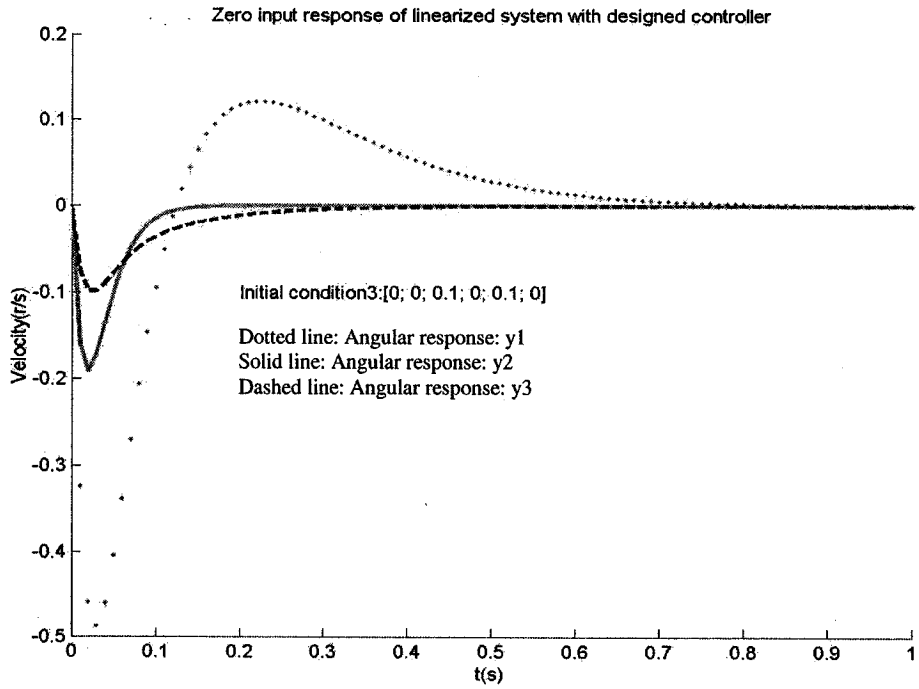

Figure 3.6. Zero input response of linearized system with initial condition1condition 3.

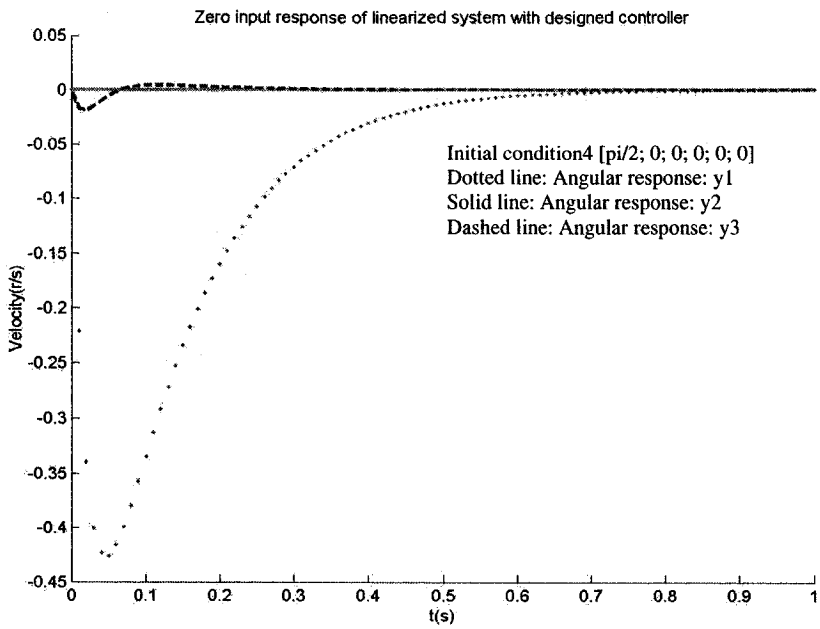

Figure 3.7. Zero input response of linearized system with initial condition 4.

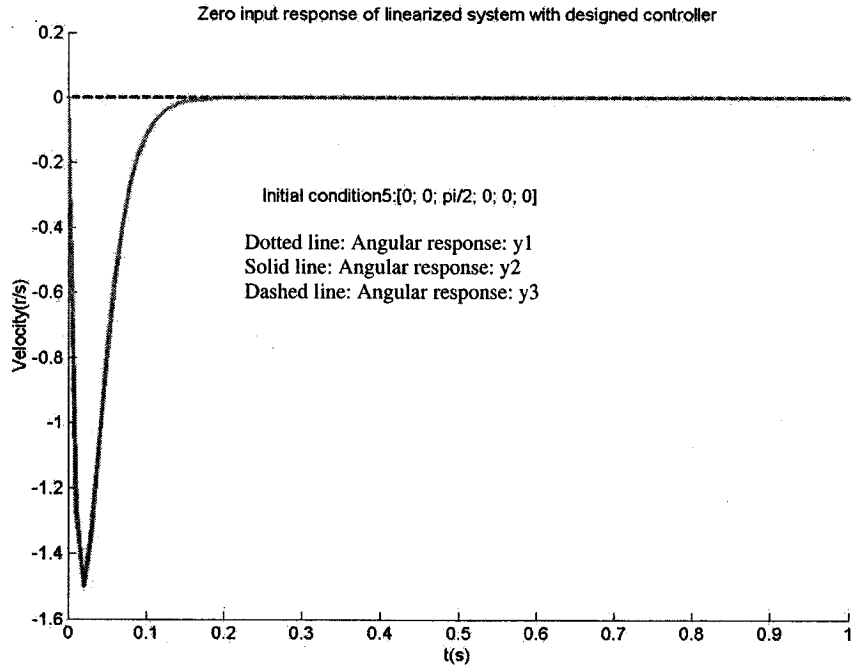

Figure 3.8. Zero input response of linearized system with initial condition 5.

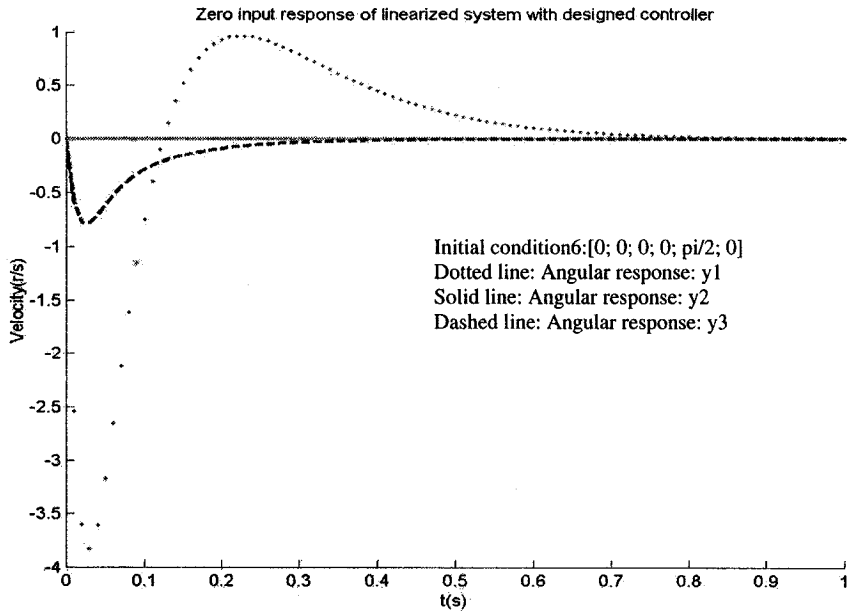

Figure 3.9. Zero input response of linearized system with initial condition 6.

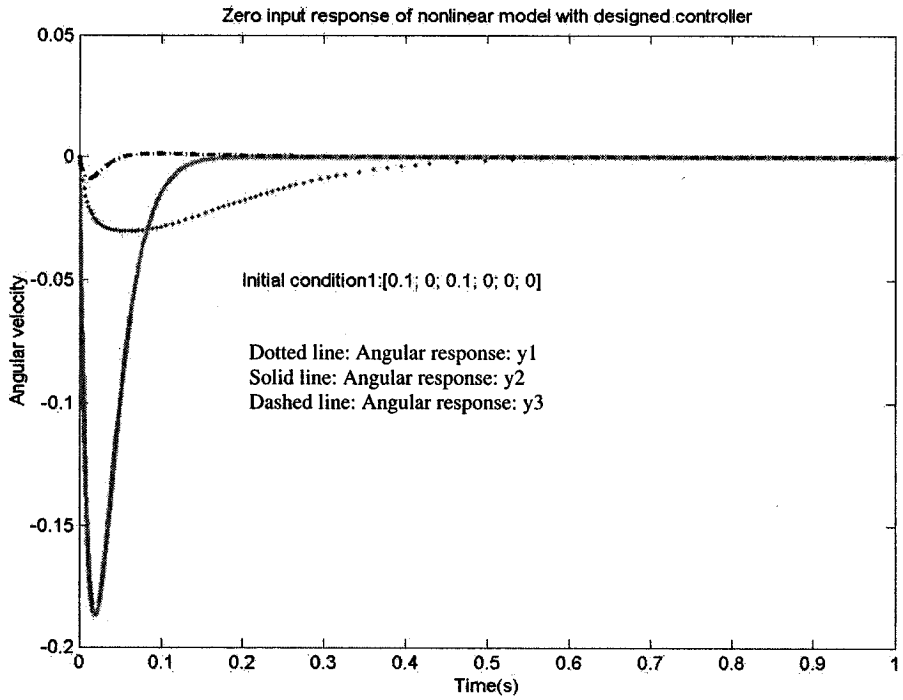

Figure 3.10. Zero input response of nonlinear system with initial condition 1.

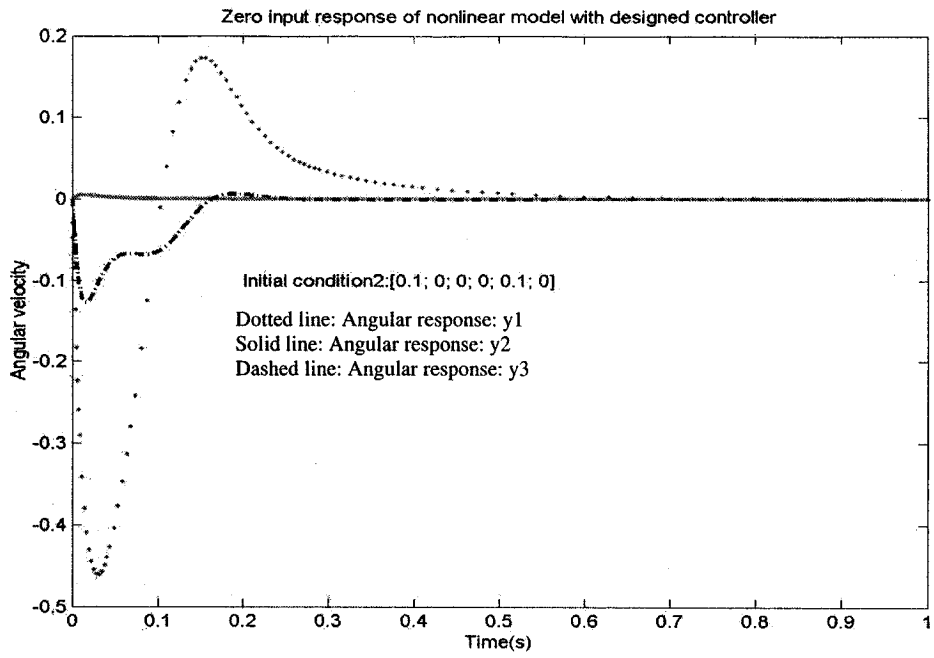

Figure 3.11. Zero input response of nonlinear system with initial condition 2.

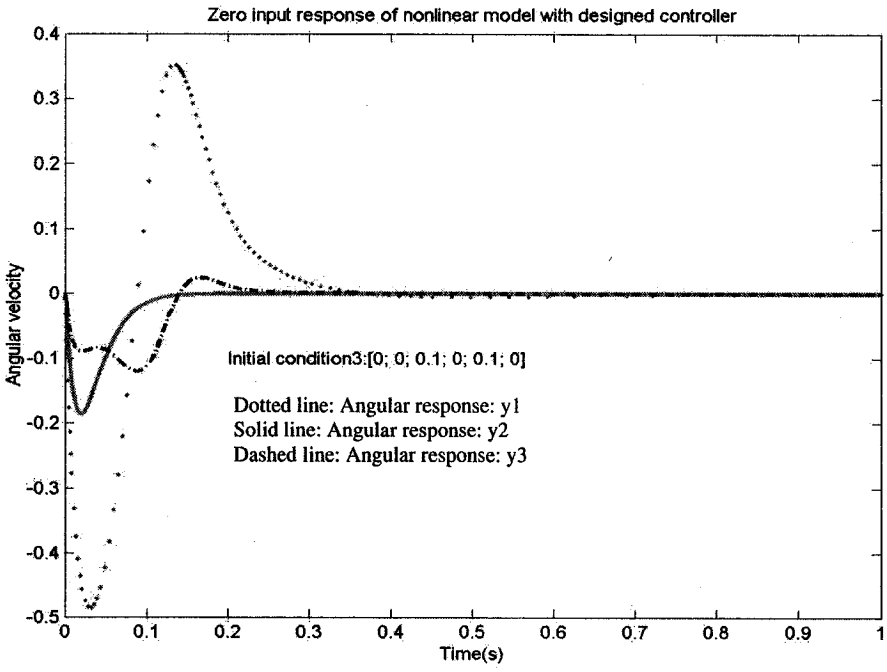

Figure 3.12. Zero input response of nonlinear system with initial condition 3.

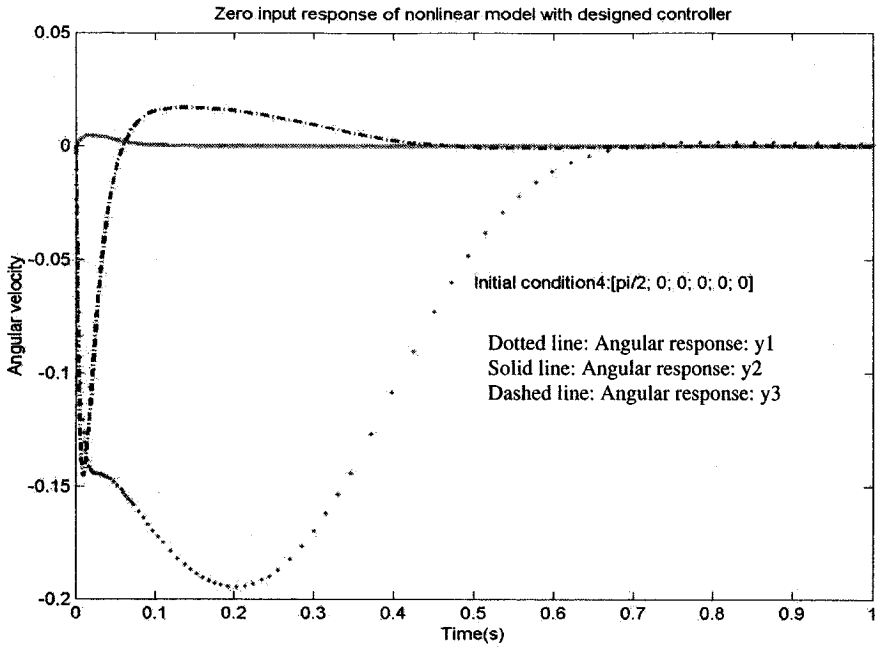

Figure 3.13. Zero input response of nonlinear system with initial condition 4.

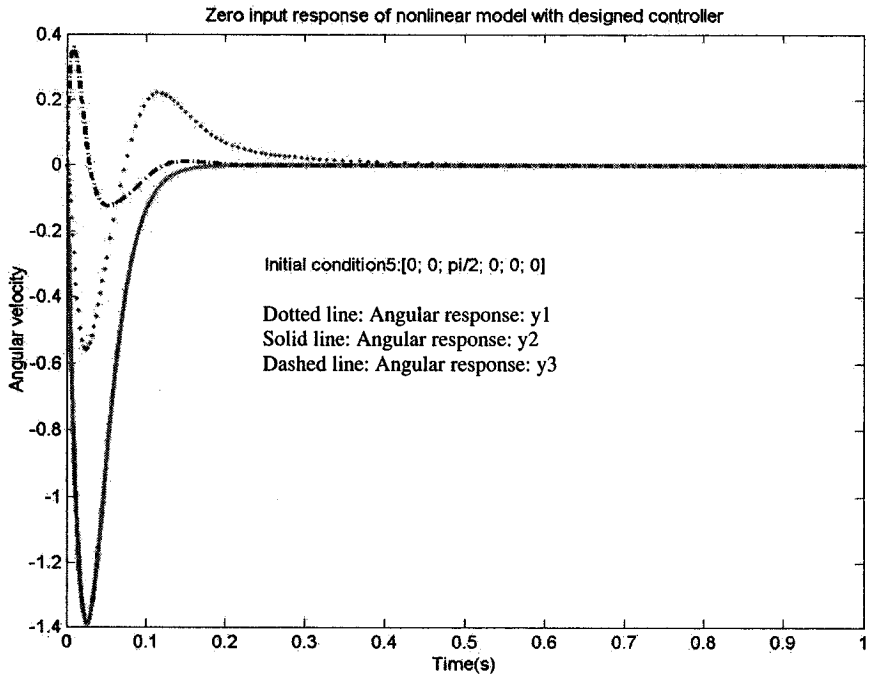

Figure 3.14. Zero input response of nonlinear system with initial condition 5.

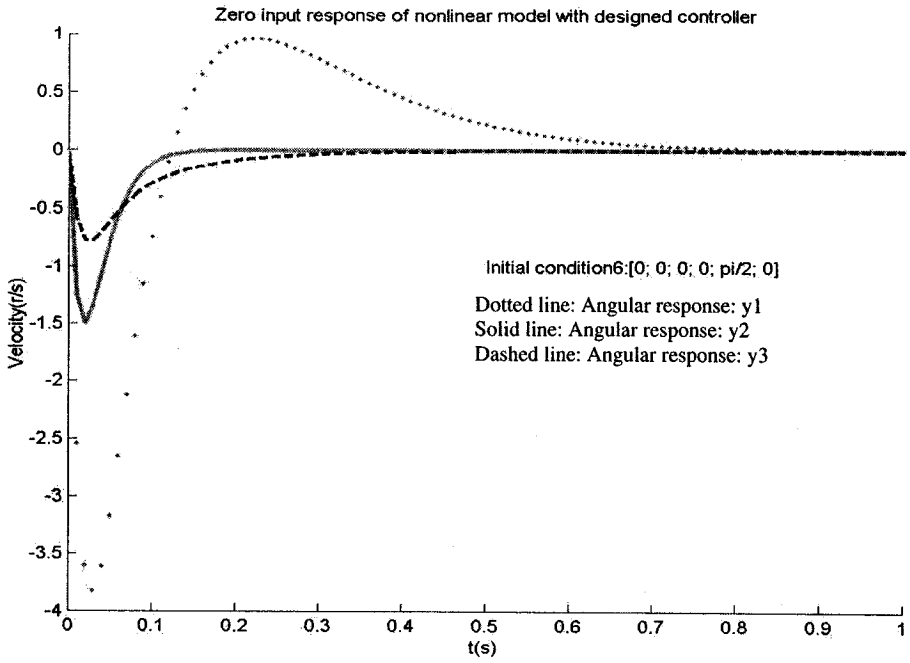

Figure 3.15. Zero input response of nonlinear system with initial condition 6.

3.5. Conclusion

In this chapter, haptic devices are introduced in general. Phantom haptic device is one of them which is a product from Sensable technology in Canbrige, MA. In order to use this Phantom haptic device to simulate the bilateral tele-operation system, we need to model the system mathematically and control the model itself as a stable subsystem.

This system model is a nonlinear model, and we need to control it and make it a stable subsystem in the bilateral tele-operation system. To achieve this, we linearized the nonlinear system at operating point [0 0 0 0 0 0], and designed a state feedback controller based on the linear control technology. To validate the effectiveness of the controller to the Phantom system, we apply this controller to the original nonlinear model. Zero input

response of both linear and nonlinear systems are investigated on different initial conditions. The simulation results show that the closed loop system is stable and can achieve their steady state in less than 1 second.

In conclusion, we can apply the designed controller to the nonlinear system and achieve a stable haptic device.

Chapter 4

Wave Variable Sliding Mode Control

for Bilateral Tele-operation System

In this chapter, wave transformation which was originally presented by [38], [39] will be used to guarantee stability of the tele-operation system which has transmission delay. However, wave transformation assumes the time delay present in the system is constant. In fact time delays rapidly fluctuate and are uncertain as in the case of the network transmission and is very non-deterministric.

Furthermore, as described earlier, the wave transformation can guarantee the stability of the communication line from the power point of view. However, this will greatly decrease the tracking precision, since the wave transformation changes the information transmitted through the communication line and no position information is transmitted through it.

Sliding-mode control is known to have tolerant characteristics to disturbances. Due to time varying nature of the system, it can be considered as disturbances to the system. Therefore, we design sliding-mode controller in the slave side to ensure the position tracking of the master and slave sides. Thus, the position floating caused by the wave transformation is resolved, and the time varying delay concern is also eliminated by the slave side controller. Therefore, the stability of the system is guaranteed as the system is now passive.

The contribution of this thesis is in combining the sliding-mode controller with that of the wave transformation theory to design a wave variable sliding mode control scheme to guarantee the stability of the time varying delay system and at the same time ensure the slave side precisely track the master position.

4.1. Simulations to Show the Effects of Delay

Before we introduce the sliding-mode control scheme, let us investigate the effects of delay by simulation. To show the effects of delay in a tele-operation system, simulations for a tele-operation system as depicted in Figure 4.1 are now conducted.

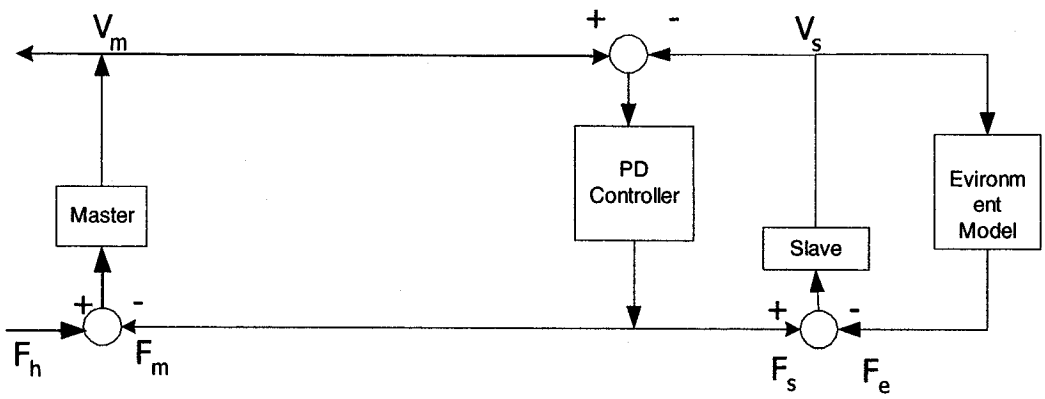

Figure 4.1. Model used to simulate the tele-operation system without delay.

For the purpose of simulations, the master side dynamic equation can be written as:

$$M_m \dot{v}_m + B_m v_m = f_h - f_m \tag{4.1}$$

The slave side dynamic equation can be written as:

$$M_s \dot{v}_s + B_s v_s = f_s - f_e \tag{4.2}$$

where M_m and M_s are the masses of the master and the slave manipulator, respectively; B_m and B_s are the viscous coefficient of the master and the slave manipulator, respectively; f_h is the force from the human operator and f_s is the force from the environment; f_e is the force from environment.

The parameters used in the above mathematical equations (according to [36], [37]) are selected as: $M_m = M_s = 0.02(kg)$ and $B_m = B_s = 0.05(Ns/m)$.

When the system has no delay, the velocity responses of the master and slave side manipulators (v_m and v_s) are shown as in Figure 4.2.

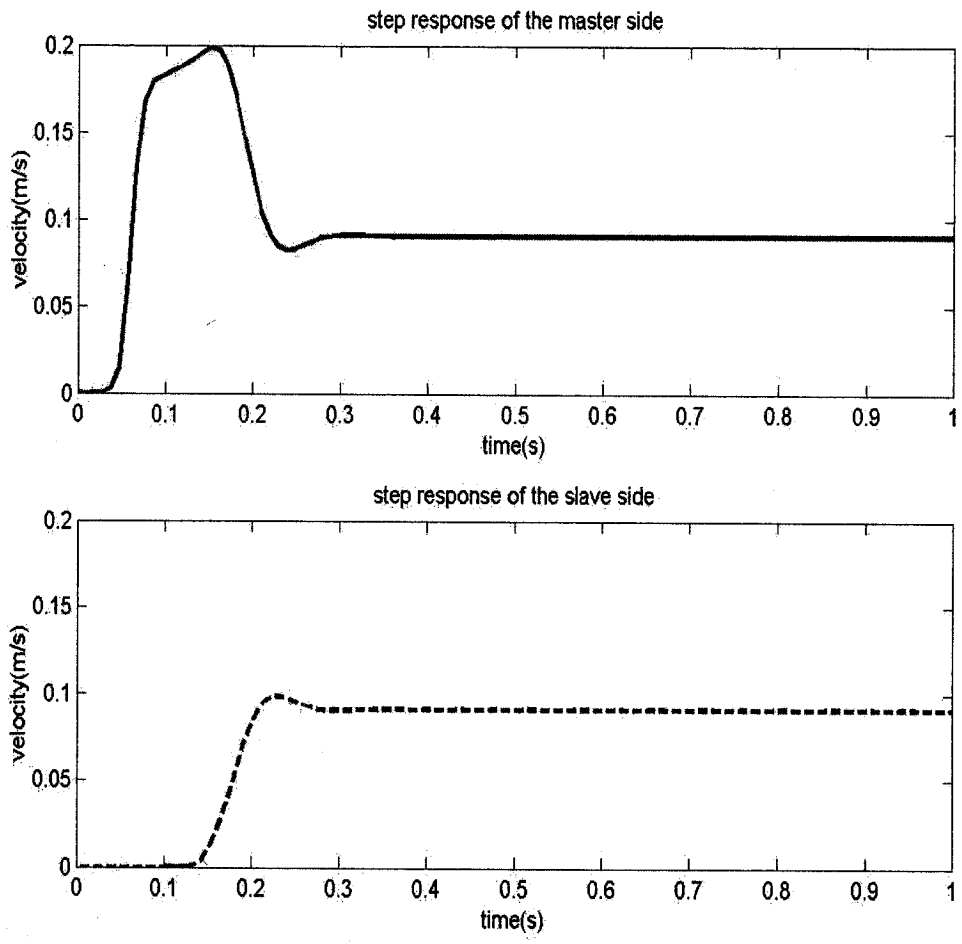

Figure 4.2. Velocity of the master and the slave when the system has no delay.

Now keeping the same parameters and only adding transmission delay of 0.5 second between the master and the slave side, as in Figure 4.3, the results for the responses are now shown as in Figure 4.4.

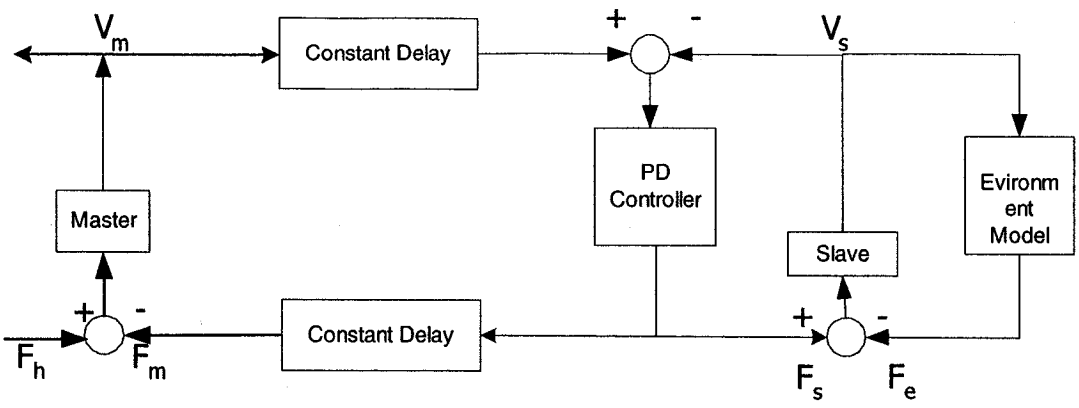

Figure 4.3. Model used to simulate the tele-operation system with 0.5s time delay.

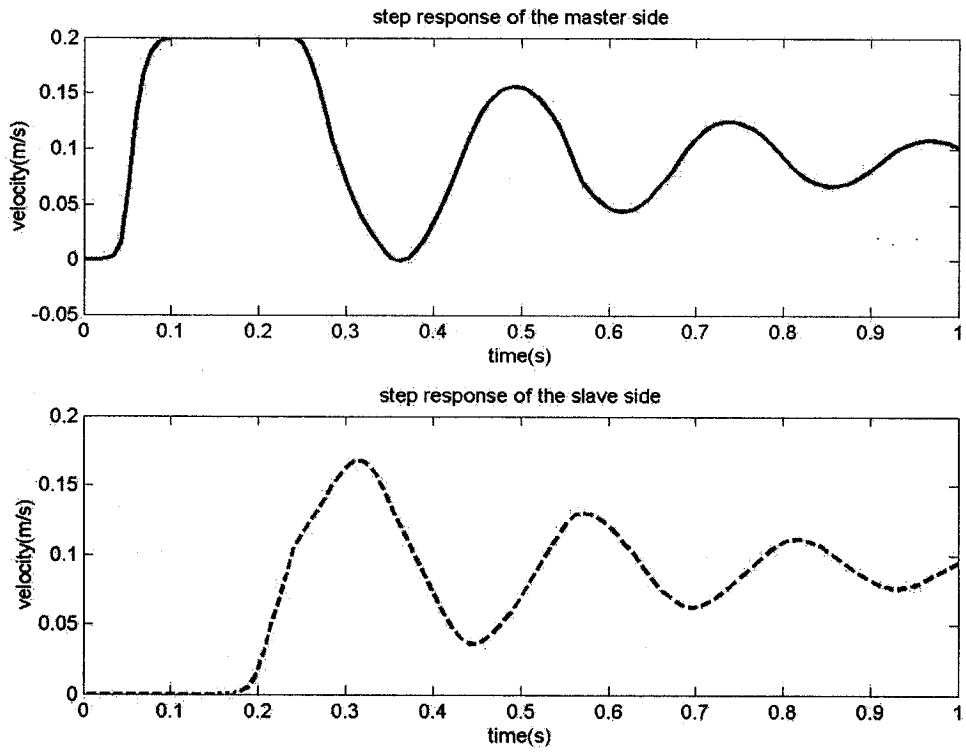

Figure 4.4. Velocity of the master and the slave when the system has 0.5s time delay.

For the tele-operation system without time delay, the velocity of the master and the slave manipulators reach their steady state values around time t = 0.25s, however, for

the system with the time delay of 0.5s, the velocity of the master and the slave oscillate and can't reach their steady state values in 1s. We can obviously observe that the time delay affects the system's stability.

4.2. Introduction to the Sliding-Mode Control [40], [41], [42], [43]

Sliding mode control is a kind of robust control. In this methodology, the high order tracking error control is simplified to the first order stability control, which is explained as follows. Consider the system

$$\frac{d^{(n)}x}{dt} = f(X) + b(X)u \tag{4.3}$$

where $X = [x \quad \dot{x} \quad \cdots \quad x^{(n-1)}]^T$ is defined as the state vector; scalar x is the output and u is the control input.

Let us define the tracking error state as:

$$X_e = X - X_d = [x_e \quad \dot{x}_e \quad \cdots \quad x_e^{(n-1)}]^T \tag{4.4}$$

where X_d is the desired trajectory and X_e is the tracking error state vector. Let us also define a time varying surface $S(X,t)$ as

$$S(X,t) = (\frac{d}{dt} + \lambda)^{n-1} x_e \tag{4.5}$$

where λ is a strictly positive constant. Actually, for X to track X_d is equivalent to that of keeping the trajectory on the surface S(t)=0 for $t > 0$.

For n=2, we obtain $S(t) = \dot{x}_e(t) + \lambda x_e(t)$ .Now, we can observe that S(t) is governed by a first order equation, and actually the solution for $S(t) \equiv 0$ is $X_e \equiv 0$ if $X_d(0) = X(0)$. The problem of tracking the n-dimensional vector X_d becomes that of keeping the first order S at zero. The first order problem of keeping the scalar S at zero can be achieved by choosing the control law u of equation (4.1) such that outside of S(t)

$$\frac{1}{2}\frac{d}{dt}S^2 \leq -\eta|s| \tag{4.6}$$

where η is a strictly positive constant. Equation (4.6) states that the squared distance to the surface, as measured by S^2, decreases along all system trajectories, once on the surface, the system trajectories remain on the surface. In other words, satisfying equation (4.6), makes the surface an invariant set. Also, equation (4.6) implies that some disturbances or dynamic uncertainties can be tolerated while still keeping the surface an invariant set, since all the trajectories outside of S will point toward S as time goes to infinity.

The concept of sliding-mode control is to choose a well-behaved function of the tracking errors S and then select the feedback control law u as in equation (4.3) such that S^2 acts like a Lyapunov function of the closed-loop system, despite the presence of model imprecision and of disturbances.

In order to satisfy the condition as presented by equation (4.6), the control law as presented in equation (4.7) has to be discontinuous across S(t), so we have

$$u = u_{eq} - k\,\mathrm{sgn}(S) \tag{4.7}$$

where u_{eq} is the control law achieved by setting $\dot{S} = 0$.

Due to the imprecision of the associated control switching, chattering occurs, which can decrease the system performance. To avoid chattering, a thin boundary layer is selected, so that inside this thin layer, the control discontinuity is smoothed out. Therefore the control law becomes

$$u = u_{eq} - ksat(\frac{S}{\varepsilon}) \tag{4.8}$$

The definition of sat(x) is given as:

$$sat(x) = \begin{cases} x & if\,|x| \le 1 \\ \mathrm{sgn}(x) & otherwise \end{cases}$$

In equation (4.8), instead of using the switching control law as in equation (4.7), signal S is filtered using a low pass filter.

4.3. Sliding-Mode Controller Design for the Slave Side

To guarantee position tracking of the slave side, a PD controller is usually deployed as in Figure 4.1. The transfer function of the controller is $\frac{Bs+K}{s}$. Since the

input signal is velocity instead of position, the integrator factor in the denominator is used. Consequently, numerical error due to the integration causes a drift between the master and slave position.

In this section, the master and slave manipulators are considered to be identical and of one degree of freedom. The master side dynamic equation can be written as in equation (4.9) and the slave side dynamic equation can be written as in equation (4.10):

$$M_m \dot{v}_m + B_m v_m = f_h - f_m \tag{4.9}$$

$$M_s \dot{v}_s + B_s v_s = f_s - f_e \tag{4.10}$$

where M_m and M_s are the masses of the master and slave manipulators respectively; B_m and B_s are the viscous coefficient of the master and slave manipulators respectively; f_h is the force from the human operator and f_m is the force reflected from slave side to the master side; and f_s are the force that will be reflected to the master side to the slave side.

Let

$$\Delta x(t) = x_s(t) - k_p x_m(t) \tag{4.11}$$

be the tracking error between the slave position and the master position. The control objective is to design a controller to make the tracking error to be zero and be maintained to be zero for all future time.

Defining the sliding surface to $z\ (t)$ as

$$z(t) = \dot{\Delta x}(t) + k_z \Delta x(t) \tag{4.12}$$

where k_z is a strictly positive constant, and according to [43], the sliding condition of

$$\frac{1}{2}\frac{d}{dt} z^2 \leq -\eta |z| \tag{4.13}$$

should be met, so that the system trajectory will move towards the sliding surface when it is off the surface.

The derivative of $z\ (t)$ with respect to time is given by

$$\begin{aligned} \dot{Z}(t) &= \dot{\Delta x}(t) + k_z \dot{\Delta x}(t) \\ &= \ddot{x}_s(t) - k_p \ddot{x}_m(t) + k_z(\dot{x}_s(t) - k_p \dot{x}_m(t)) \end{aligned} \tag{4.14}$$

Substituting equation (4.9) and equation (4.10) into equation (4.14), we get:

$$\dot{z}(t) = (k_z - \frac{B_s}{M_s}) v_s(t) + f_s(t) - f_e(t) - K_p \dot{v}_m(t) - k_p k_z v_m(t) \tag{4.15}$$

To satisfy the control objective specified above, set $\dot{z}(t) = 0$, so

$$f_s(t) = -(k_z - \frac{B_s}{M_s}) v_s(t) + f_e(t) + K_p \dot{v}_m(t) + k_p k_z v_m(t) \tag{4.16}$$

Theoretically, this controller will make the slave manipulator follow the position of the master manipulator, if the signals are transmitted from the master to the slave side

without delay. However, in a real system there is transmission delay so that the controller designed according to equation (4.16) should be modified.

Since the exact v_m is not available in the slave side, when delay exists we have to use v_{sd} in the controller instead of v_m. Thus the controller as in equation (4.16) becomes,

$$f_s(t) = -(k_z - \frac{B_s}{M_s})v_s(t) + f_e(t) + K_p \dot{v}_{sd}(t) + k_p k_z v_{sd}(t) \tag{4.17}$$

One can force the slave manipulator to follow the position of the master manipulator but with delay of T seconds. Actually, T may be time varying in a given range, and the ideal control result can not therefore be achieved. However, we can consider the variation of the time delay as perturbation to the constant time delay, and the signal variations due to this perturbation is specified as δv_d, that is

$$\tilde{v}(t) = v_{sd}(t) + k_{vd}\delta v_d(t) \tag{4.18}$$

In order to satisfy sliding condition equation (4.13) even when there is disturbance, a discontinuous term was added and equation (4.17) becomes

$$\tilde{f}_s(t) = -(k_z - \frac{B_s}{M_s})v_s(t) + f_e(t) + K_p \dot{\tilde{v}}_{sd}(t) + k_p k_z \tilde{v}_{sd}(t) \tag{4.19}$$

Now, let's verify if the controller designed according to equation (4.19) satisfies the sliding condition. From equations (4.13), (4.15) and (4.19), we have

$$\frac{1}{2}\frac{d}{dt}z^2 = \dot{z}z = k_p(\dot{v}_{sd}(t) - \dot{\tilde{v}}_{sd}(t)) - k_p K_z(v_{sd}(t) - \tilde{v}_{sd}(t))z - \beta \mathrm{sgn}(z)z$$

Assume that

$$k_v \delta v_d(t) \le k_p \max(\dot{v}_{sd} - \dot{\tilde{v}}_{sd}) + k_p k_z \max(v_{sd} - \tilde{v}_{sd}) \tag{4.20}$$

set

$$\beta = k_p \max(\dot{v}_{sd} - \dot{\tilde{v}}_{sd}) + k_p k_z \max(v_{sd} - \tilde{v}_{sd}) + \eta$$

Therefore, we have

$$\frac{1}{2}\frac{d}{dt}z^2 = \dot{z}z \le -\eta|z|$$

so that the designed controller satisfies the sliding condition.

To avoid chattering, a thin boundary layer e around the sliding surface is defined, such that $sat(\frac{z}{e}) = \begin{cases} z & if|z| \le e \\ \mathrm{sgn}(z) & if|z| > e \end{cases}$, and the controller designed in (4.19) now is given as

$$f_s(t) = (\frac{B_s}{M_s} - k_z)v_s(t) + f_e(t) + k_p \dot{v}_{sd}(t) - k_p k_z v_{sd}(t) + \beta sat(\frac{z}{\varepsilon}) \tag{4.21}$$

4.4. Introduction to the Wave Variable Theory

Before introducing the wave variable theory, let us briefly review the passivity of a two-port network.

A system with input u and output y is passive if a non-negative function W (storage function) exist, that is a function of the states (x), such that:

$$W(x(t)) \leq W(x(0)) + \int_0^t y(\tau)u(\tau)d\tau - \rho\int_0^t y^2(\tau)d\tau - \varphi\int_0^t u^2(\tau)d\tau, \forall x \in R^n, x, t \geq 0 \qquad (4.22)$$

with $\rho = \varphi = 0$. The frequency domain interpretation is that the Nyquist plot lies in the closed right half plane [44], [45].

A system with input u and output y is output strict passive if equation (4.22) is satisfied with $\varphi = 0$ and $\rho > 0$.

Output strict passivity is a stronger form of passivity. The frequency domain interpretation is that the Nyquist plot lies in a disk of radius $\frac{1}{2\rho}$.

A system with input u and output y is input strictly passive if equation (4.22) is satisfied with $\rho = 0$ and $\varphi > 0$.

Input strict passivity is a stronger form of passivity containing an excess equation to the form of passivity containing an excess equal to an amount α. The frequency domain interpretation is that the Nyquist plot lies to the right of the vertical line at φ.

The two-port network defined here is shown as in Chapter 2, Figure 2.2.

Let us define P as the "power" entering a system as the scalar product between the input vector x and the output vector y of the system. Note this power does not necessarily correspond to any actual physical power if the input/output variables are not chosen to be co-located velocity and force signals. E is defined here as an "energy storage" function, and P_{diss} is defined as "power dissipation" function.

According to the definition of passivity, the total power flow out of the system should be greater than the power flow into the system, i.e.

$$\int_0^t P d\tau = \int_0^t x^T y d\tau = E(t) - E(0) + \int_0^t P_{diss} d\tau \geq -E(0) = cons\tan t \tag{4.23}$$

The key feature of wave variables is their encoding of velocity and force information, according to

$$R = \frac{b\dot{x}_m + F_m}{\sqrt{2b}} \qquad L = \frac{b\dot{x}_s - F_s}{\sqrt{2b}} \tag{4.24}$$

Similarly the information can be decoded as:

$$\dot{x}_m = \sqrt{\frac{2}{b}} L_m + \frac{1}{b} F_m \qquad \dot{x}_s = \sqrt{\frac{2}{b}} R_s + \frac{1}{b} F_s \tag{4.25}$$

where R denotes the forward or right moving wave, and L denotes the backward or left moving wave, $\dot{x}_m$ and f_m are the velocity and force from the left side port, and $\dot{x}_s$ and f_s

are the velocity and force from the right side port. The characteristic wave impedance b is a positive constant or a symmetric positive definite matrix and assumes the role of a tuning parameter, which allows matching a controller to a particular environment or task [38], [46], [47].

From the wave variable, the power input P_{in} is given by:

$$P_{in} = \dot{x}^T F = \frac{1}{2} R^T R - \frac{1}{2} L^T L \tag{4.26}$$

when the time delay is present in the tele-operation system (refer to Figure 4.5),

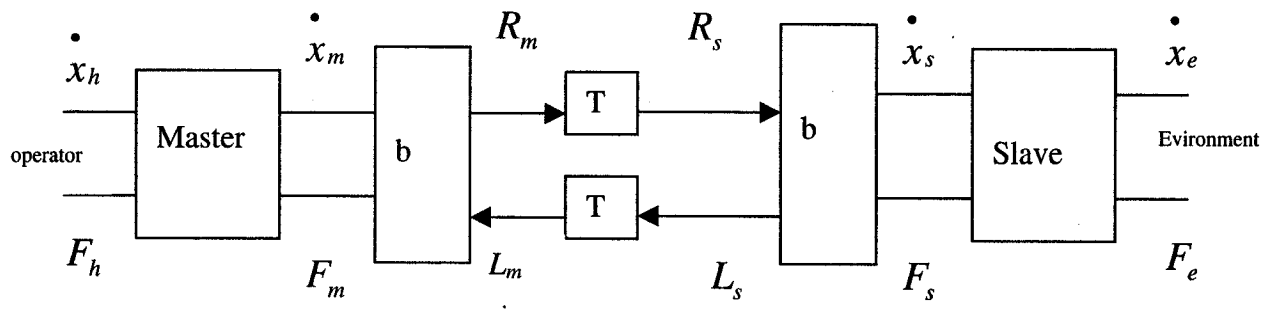

Figure 4.5. Bilateral -tele-operation system with wave variable transformation.

$$P_{in} = \frac{1}{2} {R_m}^T R_m - \frac{1}{2} {L_m}^T L_m - \frac{1}{2} {R_s}^T R_s + \frac{1}{2} L_s^T L_s \tag{4.27}$$

where $R_s(t) = R_m(t-T)$, $L_m(t) = L_s(t-T)$. By substituting R_s, L_m into equation (4.27) and integrating, we get

$$\int_0^t P_{in} d\tau = E_{store}(t) = \int_{t-T}^t \frac{1}{2} R_m^T R_m + \frac{1}{2} L_s^T L_s d\tau \geq 0 \tag{4.28}$$

The wave energy in U_m and V_s is thus temporarily stored while the waves are in transit, making the communications not only passive but also lossless. This is independent of the time delay T.

4.5. Wave Variable Sliding-Mode Control

The objective of this thesis is to design a control scheme to stabilize the tele-operation system, and at the same time ensures that the position of the slave side tracks that of the master device despite the existence of time delays in communication channel. In this thesis, we combined the sliding-mode control with the wave variable theory to archive this objective by applying the sliding-mode controller designed in section 4.3 to a wave variable transformed tele-opearation system. Wave variable transformation can guarantee the stability of the tele-operation system, and sliding-mode control can ensure the position of the slave device track that of the master device. The system can be shown as in Figure 4.6, where wave transformation is performed between the master and slave side and the sliding mode controller is used in the slave side.

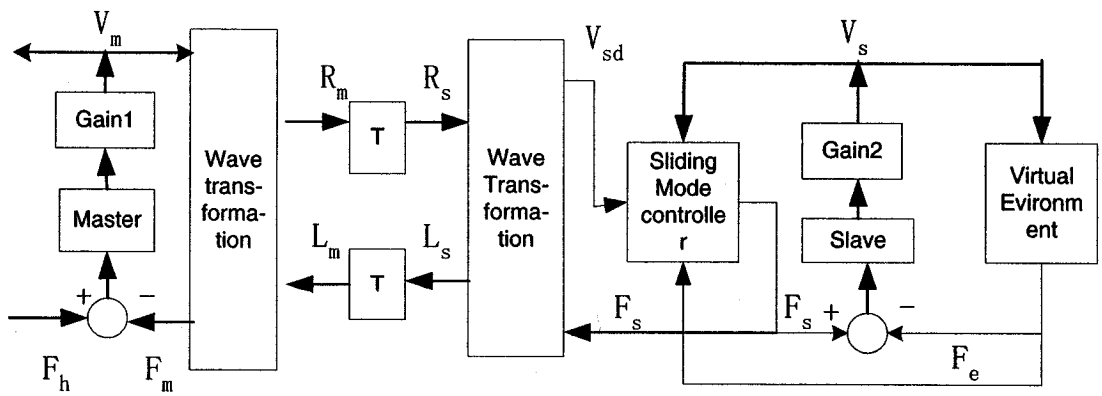

Figure 4.6. Model of tele-operation system with wave vriable sliding-mode controller.

As analyzed in this chapter section 4.2 and 4.3, sliding-mode control can ensure the position of the slave device track that of the master device at the presence of time varying delay. Now let us analysis how wave variable transformation guarantees the passivity of the tele-operation system.

The wave-based communication achieves passivity by transforming both the local and the remote information into wave variables before transmission to the other side. The wave transformation is performed as in equation (4.24), and all the variables are measured at the current time t. Note that R_m includes information of the master side velocity and feedback force at time t, and L_s includes information of slave side velocity and force at time t. Thus some delayed information is considered in R_m and L_s even before the transmission of these signals. So some terms are actually cancelled when one calculates the stored power, which can be seen clearly in the following derivations:

$$P_{in} = \dot{x}^T F = \frac{1}{2} R^T R - \frac{1}{2} L^T L \tag{4.29}$$

$$P_{in} = \dot{x}_m^T F_m - \dot{x}_s^T F_s \tag{4.30}$$

$$P_{in} = \frac{1}{2} R_m{}^T R_m - \frac{1}{2} L_m{}^T L_m - \frac{1}{2} R_s{}^T R_s + \frac{1}{2} L_s^T L_s \tag{4.31}$$

$$\int P_{in} d\tau = E_{store}(t) = \int_{-T} \frac{1}{2} R_m^T R_m + \frac{1}{2} L_s^T L_s d\tau \geq 0 \tag{4.32}$$

when one performs the integration, some terms are canceled and finally one gets equation (4.32).

In conclusion, although the system delay has no impact during the transmission, the information transmitted is different. The wave variables encode information from the other side (slave or master side) before transmission, so that the system passivity is guaranteed, thus the closed loop stability is also guaranteed.

From Figure 4.5 one can observe that, at the local (master) side, the velocity $\dot{x}_m$ and force F_m information is combined to provide a command wave signal R_m, which reaches the remote (slave) side after a delay T. There it is decoded into a velocity $\dot{x}_s$ or force F_s command. The same process returns information back to the master side.

The inherent combination of velocity and force data makes the system well suited for interaction with unknown environments. Indeed it behaves like a force controller when in contact with a rigid object and like a motion controller when in free space. The parameter b also allows online trade-off between the two quantities by fine tuning the behavior.

In summary, the wave variable transformation process is like a controller with parameter b, which will guarantee the passivity of the Tele-operation system. However, simulation results show [46] that when time delay is longer, the system performance degrades, and when the time delay varies, the slave side can not well track the position of the master side. As analyzed in sections 4.2 and 4.3, sliding-mode control is robust to disturbance, and if we can consider the time varying delay as a disturbance to a constant time delay, the tracking issue can be resolved by applying the designed sliding-mode controller to the slave side of the system.

4.6. Conclusion

In this chapter, wave variable control is introduced, and a wave variable transformation subsystem is designed for the tele-operation system that we have established. Furthermore the sliding mode control is also reviewed, and a sliding mode controller is designed for the slave side based on the system parameters. The wave variable sliding mode controller will be applied to the system and simulation will be conducted in the next chapter.

Chapter 5

Comparison of Wave Variable Sliding Mode Control with the Conventional Wave Variable Control Strategy

In this chapter, the proposed wave variable sliding mode control strategy is compared with the conventional wave variable control method. The comparison is performed by simulating both control strategies and analyzing the simulation result based on the same initial conditions [48], [49], [50], [51], [52], [53], [54], [55].

5.1. Simulation Results

The simulation parameters are selected according to [36]

$$M_m = M_s = 0.02(kg)$$

$$B_m = B_s = 0.05(Ns/m)$$

with the adjustment gain for the master and slave transfer function is set as 0.01, and the force input used in this simulation is a uniform random signal. For the wave transformation approach, b=0.2, and in the sliding mode controller, $k_p = k_z = 1, \beta = 0.1$ and $\varepsilon = 0.01$.

In the simulation result, the white noise signal is added to a constant delay to simulate the variable time delay. The white noise signals used are shown in Figure 5.3a and 5.3b. We define the white noise shown in Figure 5.3a as W1 and that shown in Figure 5.3b as W2. In W1, the maximum value is 0.1 and in W2 the maximum value is 0.18.

The conventional wave variable control system is depicted as in Figure 5.1 and the wave variable sliding mode control system is depicted as in Figure 5.2. For the system depicted in Figure 5.1, a PD controller is designed in the slave side. When the time delay is 250ms, and a band limited white noise signal *W1* is added to the delay signal as a disturbance, the simulation result of the position response is shown as in Figure 5.4a. In contrast, the simulation result of the position response of the wave variable sliding mode control system is shown as in Figure 5.4b. When we change the

time delay from 500ms to 1s and keep the same noise signal, the simulation results for the two systems are given in Figures 5.5a, 5.5b, 5.6a, and 5.6b. When the time delay is 500ms and the white noise is increased to 0.0003, the simulation results are shown as in Figures 5.7a and 5.7b.

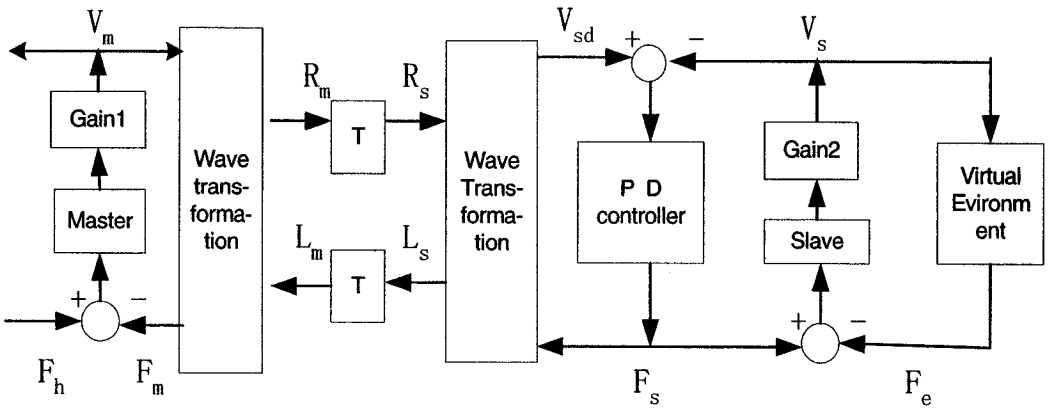

Figure 5.1. Conventional wave variable control system.

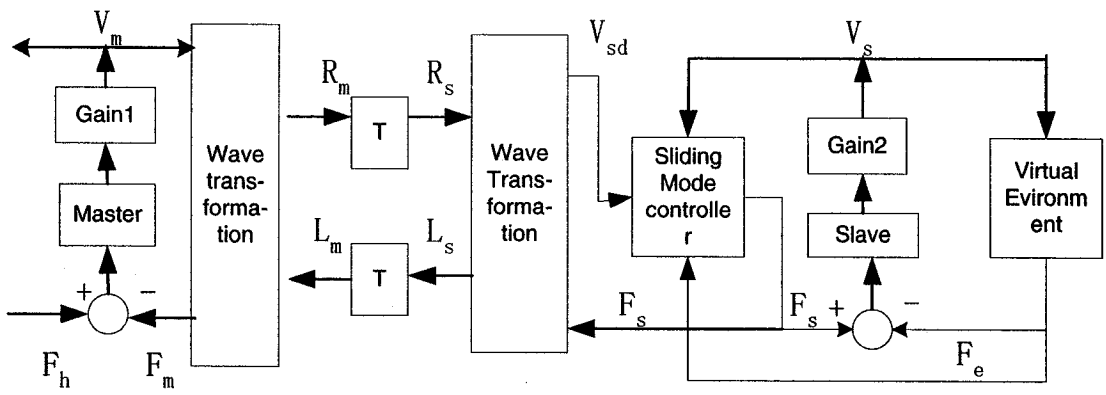

Figure 5.2.Wave variable sliding mode control system.

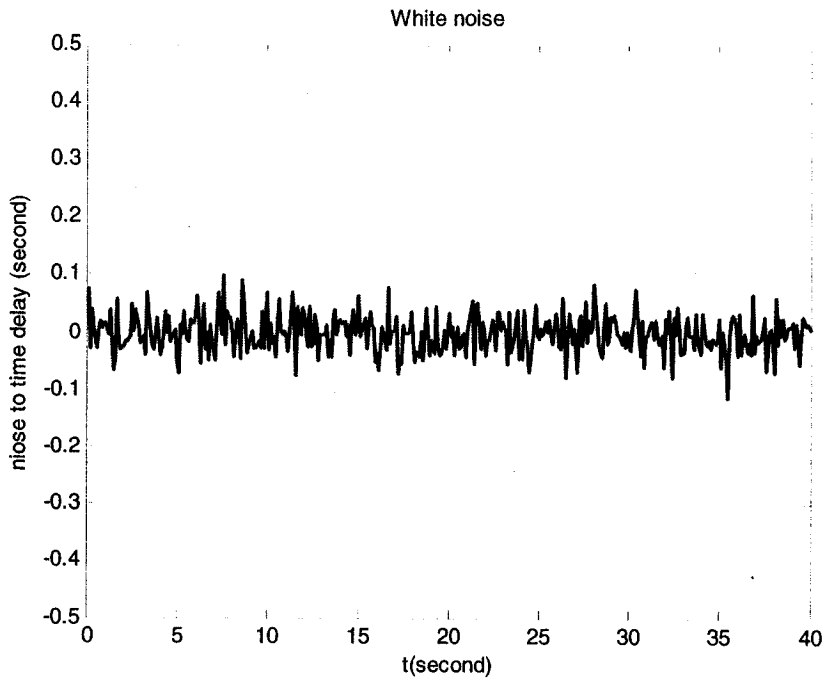

Figure5.3a. White noise with power of 0.0001.

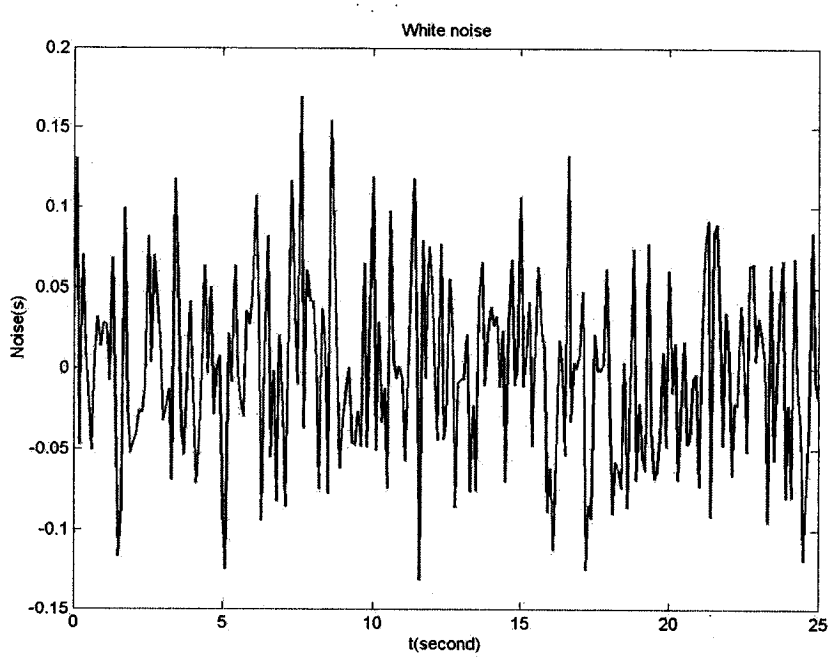

Figure 5.3b. White noise with power of 0.0003.

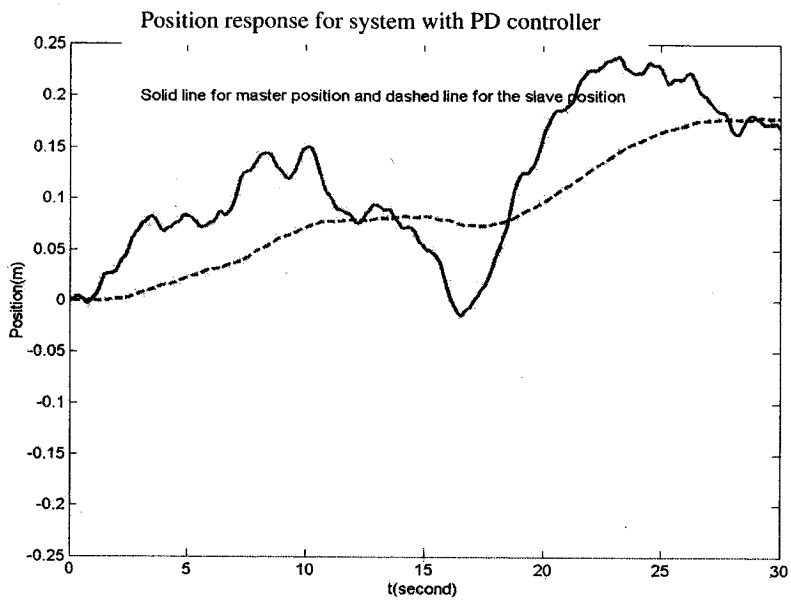

Figure 5.4a. The position response with PD controller (solid line for the master side and the dashed line for the slave side), T=250ms, white noise power=0.0001.

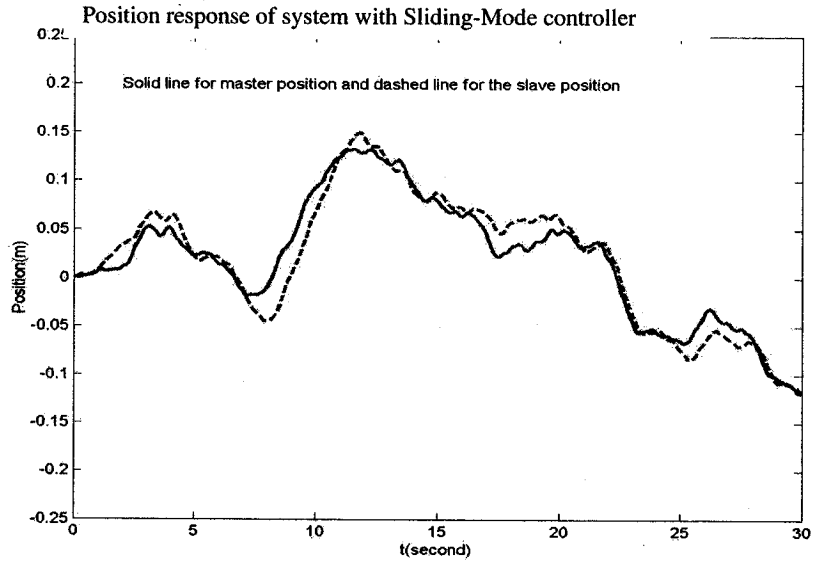

Figure 5.4b. The position response with sliding mode controller (solid line for the master side and the dashed line for the slave side), T=250ms, white noise power=0.0001.

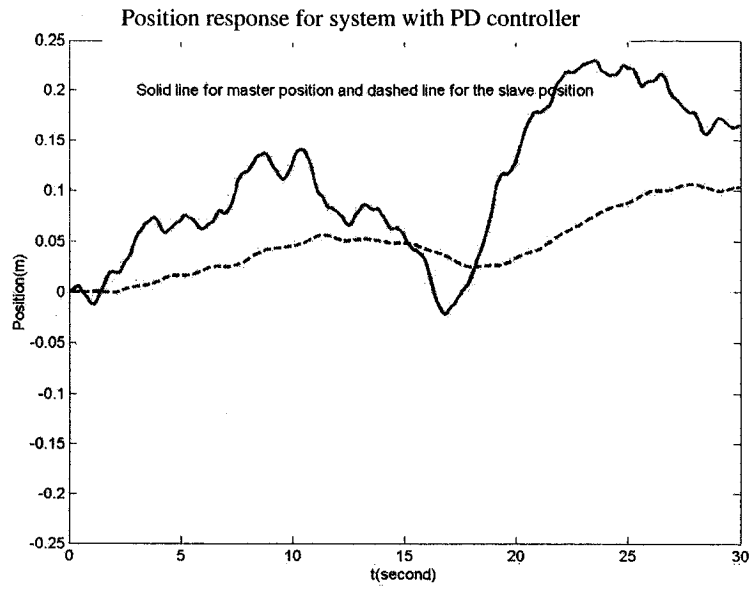

Figure 5.5a. The position response with PD controller (solid line for the master side and the dashed line for the slave side), T=500ms, white noise power=0.0001.

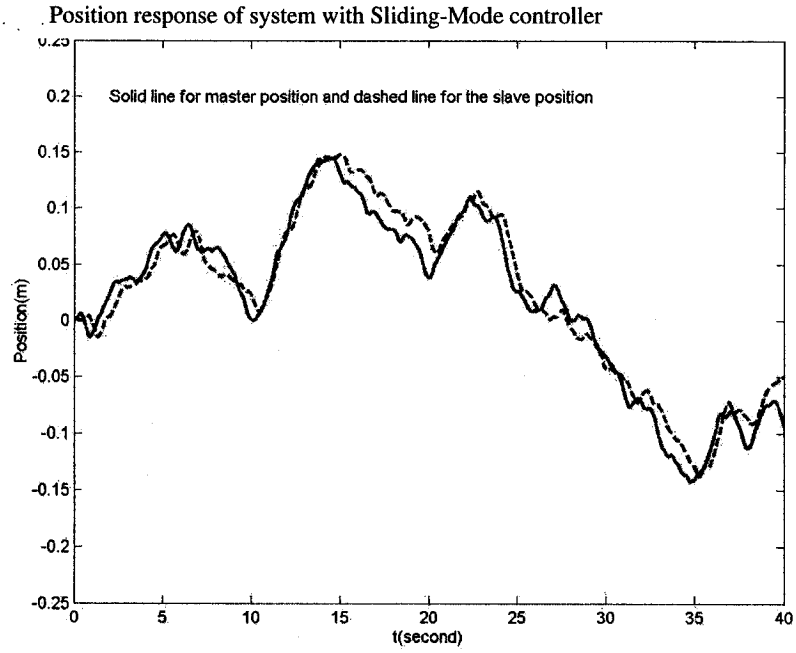

Figure 5.5b. The position response with sliding mode controller (solid line for the master side and the dashed line for the slave side), T=500ms, white noise power=0.0001.

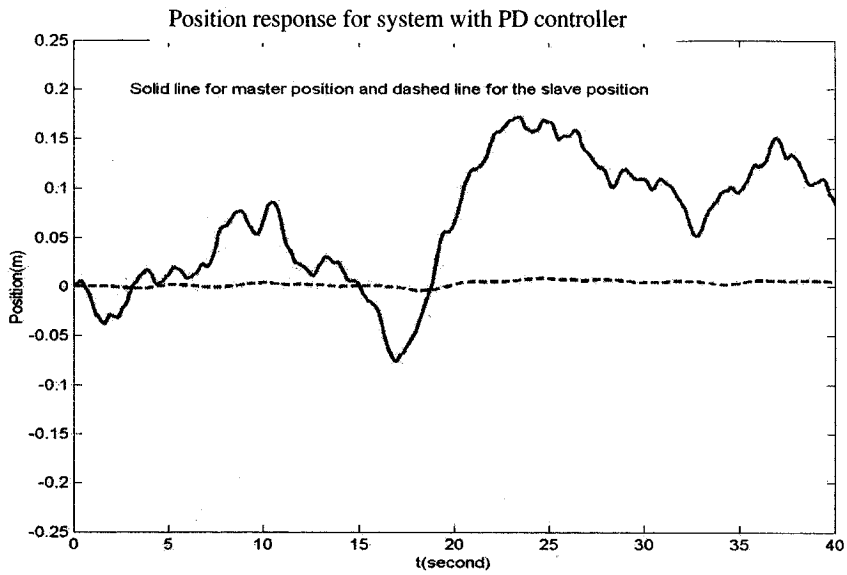

Figure 5.6a. The position response with PD controller (solid line for the master side and the dashed line for the slave side), T=1s, white noise power=0.0001.

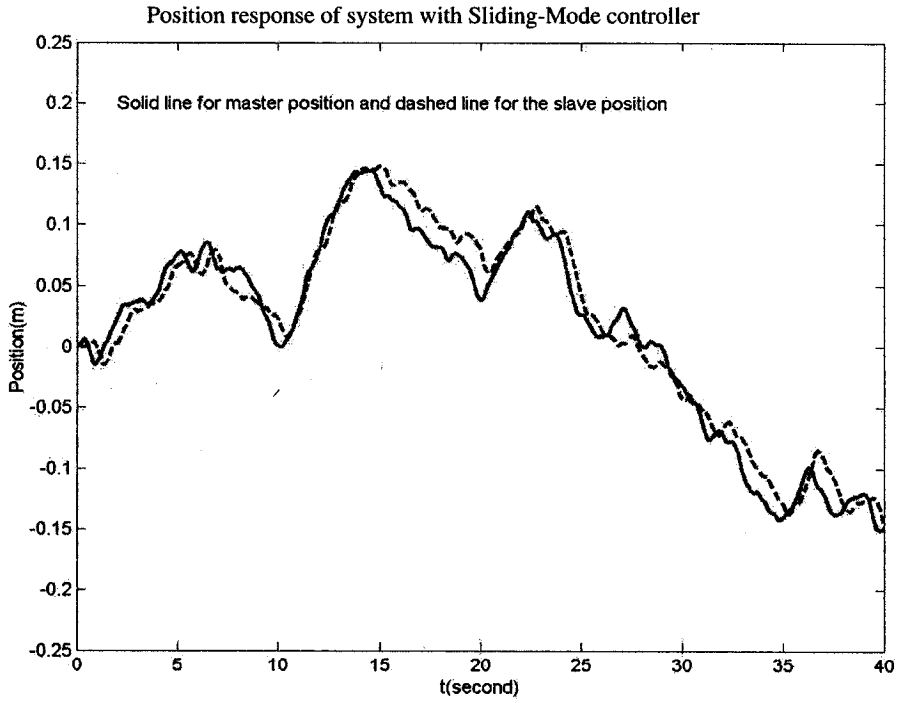

Figure 5.6b. The position response with sliding mode controller (solid line for the master side and the dashed line for the slave side), T=1s, white noise power=0.0001.

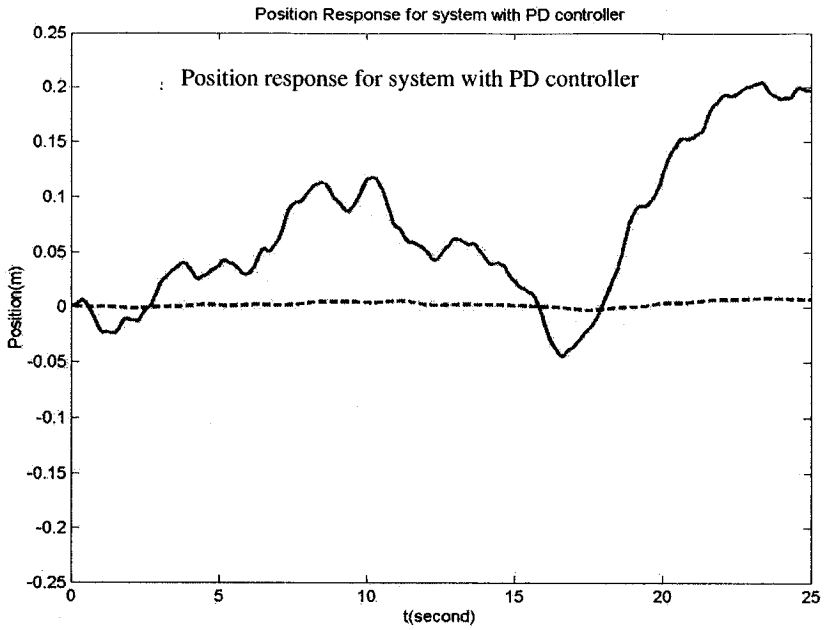

Figure 5.7a. The position response with PD controller (solid line for the master side and the dashed line for the slave side), T=500ms, white noise power is 0.0003.

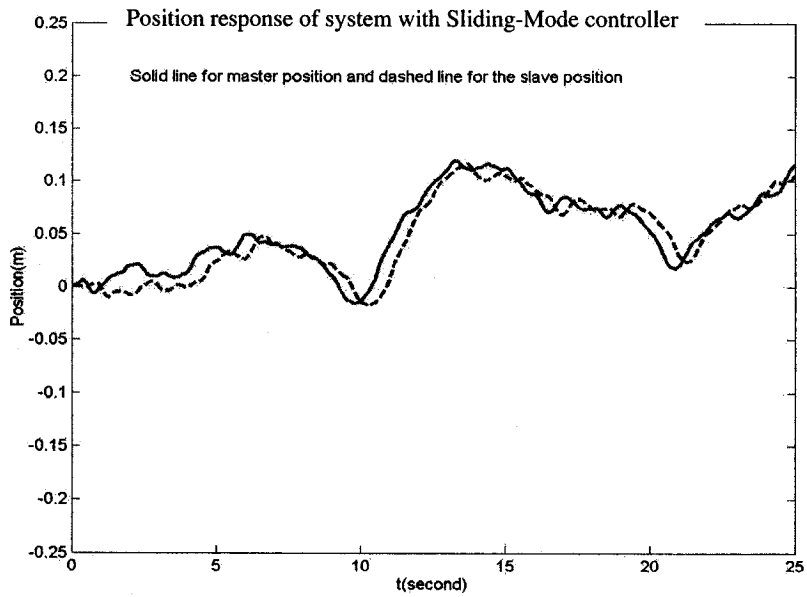

Figure 5.7b. The position response with sliding mode controller (solid line for the master side and the dashed line for the slave side), T=500ms, white noise power is 0.0003.

In the following table, the tracking error of the master and slave position is compared between the wave variable sliding mode control system and the conventional wave variable system. From the table we can observe that when time delay is varying, which is simulated as a constant time delay plus a white noise signal, the performance of the conventional wave variable control is not desirable, the tracking error is more than 10% when time delay is less 1s and white noise signal is limited by 0.1 s maximum.

Dealy(s) / Controller	D=0.25s W1	D=0.5s W1	D=1s W1	D=0.5s W2
Wave variable sliding mode control	**0.0135**	**0.0138**	**0.0152**	**0.0156**
Conventional wave variable control	**0.1212**	**0.1316**	**0.1415**	**0.1618**

From the table we can observe that when time delay is varying, which is simulated as a constant time delay signal plus a white noise signal, the tracking error of system with the wave variable sliding mode control was reduced significantly compared to system with the conventional wave variable control.

When time delay is less than 1s and white noise signal is limited by 0.1s maximum, the tracking error is 13% on average. In contrast, the tracking error of the

wave variable sliding mode control is 1.4% on average, which reduces the tracking error by 89%.

By retaining the same varying factor of the time delay, that implies keeping the same white noise signal in the simulations, and increasing the constant time delay factor from 0.25s to 0.5s, the tracking error for conventional wave variable control is increased by 0.01 and that of wave variable sliding mode control is increased by 0.0003 which means the system with wave variable sliding mode controller is less sensitive to the increase of the amount of time delay than the system with conventional wave variable controller.

By retaining the same constant factor of the time delay as 0.5 s and increasing the maximum value of the white noise signal from 0.1s to 0.18s, the tracking error of the conventional wave variable control is increased by 0.03, and that of the sliding mode control is increase by 0.0018, which implies that with the presence of varying time delay the later approach is much more robust to time varying factor.

5.3. Conclusion

In this chapter, wave variable sliding mode control and conventional wave variable control are simulated. The results are shown in Figures 5.4a to 5.7b and are compared. From the results we can observe that the wave variable control scheme is much more robust to the tele-operation system when the time delay is varying, when compared with the conventional wave variable method. Using a comparison matrix shown above, we can observe that the tracking error is reduced in general by 90%.

Wave variable transformation, as analyzed in Chapter 4, has the nature of retaining passivity of the tele-operation system. However, as mentioned in [24], this comes at the expense of degraded performance, the larger the time delay, the longer it takes to accomplish a given task, in other words, it takes longer time for the system to stabilize, which causes large tracking errors. Also, when time delays vary, the performance of the system degrades using the conventional wave variable control scheme. However, for the wave variable sliding mode control scheme, the sliding mode control can compensate this problem since it is naturally capable of controlling these issues at the presence of disturbances.

Chapter 6

Conclusions and Future Research

In this chapter, the research work and simulation results are concluded and future research directions are listed as follows.

6.1 Conclusions

In this thesis, stability of a bilateral tele-operation system is analyzed. In Chapter 1, issues present in the tele-operation are reviewed, and the problem that this thesis is

concerned with, which is the stability issue caused by communication time delay is highlighted. In Chapter 2, tele-operation charicteristics and virtual reality based tele-operation are reviewed. Again, stability issue is emphasized, and current solutions to this problem are reviewed, which include the scattering theory, Smith predictor based control theory, and model based theory. Although these methods could solve the stability problems to some extend, they have few limitations. Controller designed based on scattering theory can not perform well when the delay is time varying, and Smith prediction methods are based on linear system theory which cannot work well for nonlinear systems. In addition, Smith prediction and model based theory need precise system modeling, which is quite hard to achieve in most of the cases.

In Chapter 3, the model of a phantom haptic device is investigated. The nonlinear system model is linearized around an equilibrium point, and a state feedback controller is designed to guarantee the stability of the haptic device. Furthermore, the controller is applied to the nonlinear system in simulations to validate the efficiency of the controller for a nonlinear system. The results show that the controller works quite well on the nonlinear system subject to different initial conditions.

The model of the tele-opeation system with phantom haptic device is introduced and stability property of this system is analyzed in Chapter 4. Wave transformation method is applied for this system and also sliding mode controller is designed for the tele-operation system. Wave transformation is an attractive method for tele-operation systems with time delay, since it can guarantee the passivity of the communication channel regardless of the time delay. However, this method introduces position tracking

problems. Position tracking performance cannot be satisfied in general. The sliding-mode controller designed in this thesis improves the resulting tracking performance results. The simulation results verify and illustrate the observation that the position tracking error bounds are improved noticeably. In order to test the robustness of the designed control system, time varying transmission delays are also considered by treating the delay variations as white noise added to a constant delays. The results show that when the maximum value of the white noise is less than 50% of the constant delay, the tracking error is within 1.56%.

6.2. Future Work

1. The designed control scheme can be put into an experimental system for further implementation and testing. The experimental system can be set up with master Phantom haptic device connected to the master computer system and the slave Phantom haptic device connected to the slave computer system. The slave side environment can be simulated with a virtual environment.
2. The stability theory regarding the time varying telecommunication delay can also be further investigated based on the nature of the network. For example, the effect of the variable network latency can be further modeled and investigated and the effect of the network peak latency can also be further considered. Also, the network architecture itself also affects the behavior of the time varying delay. The delay of the network can be modeled and control of the tele-operation system can be further investigated.

3. Further research deserves to be performed on the stability issue of a multi-user collaborated tele-operation system, especially via Internet. The nature of the time delay caused by Internet needs to be investigated, which implies that one needs to know more about the network and communication protocols.

Appendix 1

$$M_{11} = (\frac{1}{8}(4I_{ayy} + 4I_{azz} + 8I_{baseyy} + 4I_{beyy} + 4I_{bezz} + 4I_{cyy} + 4I_{czz} + 4I_{dfyy} + 4I_{dfzz} + 4l_1^2 m_a$$
$$+ l_2^2 m_a + l_1^2 m_c + 4l_3^2 m_c) + \frac{1}{8}(4I_{beyy} - 4I_{bezz} + 4I_{cyy} - 4I_{czz} + l_1^2(4m_a + m_c))\cos(2\theta_2)$$
$$+ \frac{1}{8}(4I_{ayy} - 4I_{azz} + 4I_{dfyy} - 4I_{dfzz} - l_2^2 m_a - 4l_3^2 m_c)\cos(2\theta_3)$$
$$+ l_1(l_2 m_a + l_3 m_c)\cos(\theta_2)\cos(\theta_3))$$

$$M_{22} = \frac{1}{4}(4(I_{bexx} + I_{cxx} + l_1^2 m_a) + l_1^2 m_c)$$

$$M_{23} = \frac{1}{2} l_1(l_2 m_a + l_3 m_c)\sin(\theta_2 - \theta_3)$$

$$M_{33} = \frac{1}{4}(4I_{axx} + 4I_{dfxx} + l_2^2 m_a + 4l_3^2 m_c)$$

$$C_{11} = \frac{1}{8}(-2\sin(\theta_2)((4I_{beyy} - 4I_{bezz} + 4I_{cyy} - 4I_{czz} + 4l_1^2 m_a + l_1^2 m_c)\cos(\theta_2)$$
$$+ 2l_1(l_2 m_a + l_3 m_c)\sin(\theta_3))\dot{\theta}_2 + 2\cos(\theta_3)(2l_1(l_2 m_a + l_3 m_c)\cos(\theta_2)$$
$$+ (-4I_{ayy} + 4I_{azz} - 4I_{dfyy} + 4I_{dfzz} + l_2^2 m_a + 4l_3^2 m_c)\sin(\theta_3))\dot{\theta}_3)$$

$$C_{12} = -\frac{1}{8}((4I_{beyy} - 4I_{bezz} + 4I_{cyy} - 4I_{czz} + l_1^2(4m_a + m_c))\sin(2\theta_2)$$
$$+ 4l_1(l_2 m_a + l_3 m_c)\sin(\theta_2)\sin(\theta_3))\dot{\theta}_1$$

$$C_{13} = -\frac{1}{8}(-4l_1(l_2 m_a + l_3 m_c)\cos(\theta_2)\cos(\theta_3)$$
$$- (-4I_{ayy} + 4I_{azz} - 4I_{dfyy} + 4I_{dfzz} + l_2^2 m_a + 4l_3^2 m_c)\sin(2\theta_3))\dot{\theta}_1$$

$$C_{21} = -C_{12}$$

$$C_{23} = \frac{1}{2}(l_1(l_2 m_a + l_3 m_c)\cos(\theta_2 - \theta_3)\dot{\theta}_3)$$

$$C_{31} = -C_{13}$$

$$C_{32} = \frac{1}{2} l_1(l_2 m_a + l_3 m_c)\cos(\theta_2 - \theta_3)\dot{\theta}_2$$

$$N_2 = \frac{1}{2} g(2l_1 m_a + 2l_5 m_{be} + l_1 m_c)\cos(\theta_2)$$

$$N_3 = \frac{1}{2} g(l_2 m_a + 2l_3 m_c - 2l_6 m_{df})\sin(\theta_3)$$

Where, *l*, *m*, *I* are parameters of the phantom haptic device.

Bibliography

1. Adam J. A.; "Probing beneath the sea", IEEE Spectrum, April; 55-64,1985
2. Butler A. Y., Rickey W. P.; "Operation Status of Diverless Work System"; Oil and Gas Journal, Vol. 80, Num. 25; 216-236; 1982
3. Grimson, W., Lozano-Perez, T., and Wells ,W.; "An automatic registration method for frameless stereotaxy, image guided surgery and enhanced reality; IEEE Conference on Computer Vision and Pattern Recognition Proceedings, Los Alamitos, CA; 430-436; 1994
4. Bejczy A. K., Venema S., Kim W. S.; "Role of Computer Graphics in Space Telerobotics: Preview and Predictive Displays; SPIE Volume 1387 Cooperative Intelligent Robotics in Space"; 365-377; 1990
5. http://www.ece.ubc.ca/~tims/bg_tel.html, Some back ground on tele-operation and haptic interface. Accessed Jan, 2006.
6. http://vehand.engr.ucf.edu/handbook/Chapters/Chapter56/kay.html, Virtual reality assisted tele-operation. Accessed Jan, 2006.
7. Hirzinger G., Brunner B., Dietrich J., Heindl J.; "Sensor-Based Space Robotics - ROTEX and Its Telerobotics Features"; IEEE Transactions on Robotics and Automation, Vol. 9, Number 5; 649-663; 1993
8. Dunbar R. M., Klevelant H., Lexander J., Svensson S., Tennant A. W.; "Autonomous underwater vehicle communications"; ROV `90, The Marine technology Society, 270-278, 1990

9. Sheridan T. B.; "Telerobotics, Automation and Human Supervisory Control"; MIT Press; 1992

10. Hayati S., Venkataraman S. T.; "Design and Implementation of a Robot Control System with Traded and Shared Control Capability"; Proceedings IEEE International Conference on Robotics and Automation; 1310-1315,1989;

11. Sturges R. H. J.; "Reliability and Safety in Tele-operation; Safety, Reliability and Human Factors in Robotic Systems", Ed. J. H. Graham, New York: Van Nostrand Reinhold; 83-115; 1991

12. Peters S. F.; "Autonomy through interaction: the JPL telerobot interactive planning system"; SPIE Volume 1006 Space Station Automation IV; 173-178; 1988.

13. Burtnyk N., Greenspan M. A.; "Supervised Autonomy - Partitioning Telerobotic Responsibilities Between Human and Machine"; International Conference on Intelligent Tele-operation, Nov 6-7; 34-42; 1991

14. Ferrell W. R., Sheridan T. B.; "Supervisory control of remote manipulation"; IEEE Spectrum, October; 81-88; 1967

15. Elhajj, I.; Xi, N.; Wai Keung Fung; Yun Hui Liu; Li, W.J.; Kaga, T.; Fukuda, T.; "Haptic information in Internet-based tele-operation", IEEE/ASME Transactions on Mechatronics, Volume: 6, Issue: 3, 295 – 304, Sept. 2001

16. http://vered.rose.utoronto.ca/people/anu_dir/thesis/fchp1.fm.html, Introduction to tele-operation. Accessed Jan, 2006.

17. http://www.iha.tut.fi/education/IHA-3500/files/Teleoperation_Notes.pdf. Tele-opetation. Accessed Jan, 2006.

18. Burdea, G.C.; "Haptics issues in virtual environments", International Proceedings of Computer Graphics, 295 – 302, 19-24 June 2000.

19. Jennings, C.; "Cooperative Robot Localization With Vision-based Mapping"; Proceedings of the IEEE International Conference on Robotics and Automation Detroit, Michigan. May 1999.

20. Cavusoglu, M.C.; Feygin, D.; "Kinematics and Dynamics of Phantom(TM) Model 1.5 Haptic Interface", Technical report, 2001.

21. Kosuge, K.; Hashimoto, S.; Yoshida, H.; "Human-robots collaboration system for flexible object handling", Proceedings, IEEE International Conference on Robotics and Automation, Volume: 2 , 1841 – 1846,16-20, May 1998 .

22. Sheridan T. B.; "Tele-operation, Telepresence, And Telerobotics: Research Needs for Space"; NAS/NASA Symposium on Space Station Human Factors, Jan 1987.

23. Dai, F.; "Virtual reality for industrial applications", Berlin ; New York : Springer, 1998

24. Munir, S.; Book, W. J.; "Wave-based tele-operation with prediction", Proceedings of the American control conference Arington, VA June 25-27, 2001.

25. Buttolo, P.; Oboe, R.; Hannaford, B; "Architecture for Shared Haptic Virtual Environments", Computer and Graphics, Vol, 21, No. 4, 421-429, 1997.

26. Gossweiler, R., Laferriere, R. J., Keller, M. L. and Pausch, R. "An introductory tutorial for developing multiuser virtual environments". PRESENCE, 3(4), 225-264, 1994.

27. Buttolo, P., Kung, D. and Hannaford, B.; "Manipulation in real remote and virtual environments. In Proceedit"; IEEE Conference on Systwns, Man. And Cyhernetrcs. 1995.

28. http://www.sensable.com. Accessed, Jan, 2006.

29. Das H., Sheridan T. B., Slotine J. E.; "Kinematic Control and Visual Display of Redundant Teleoperators"; Proceedings of International Conference on Systems, Man and Cybernetics, Vol. 3, Nov. 14-17; 1072-1077; 1989

30. Lin, Q. P. and Frse, F.; "Virtual tele-operation of underwater robots", Proceedings of the IEEE International Conference on Robotics and Automation, 1022-1027. Albuquerque, New Mexico, Apr. 1997.

31. Anderson, R. J.; "Bilateral Control of Teleoperators with Time Delay", IEEE Transaction on Automatic Control, Vol. 34, No. 5, May 1989.

32. Arioui, H., Mammar, S. and Hamel, T. "A smith-prediction based haptic feedback controller for time delayed virtual environments systems", Proceedings of the American Control Conference, Anchorage, AK, May, 2002.

33. Arioui, H., Kheddar, A. and Mammar, S. "A model-based controller for interactive delayed haptic feedback virtual environements", Journal of Intelligent and Robotic Systems, vol. 37: 193-207, 2003.

34. Adams, R. and Hannaford, "Stable Haptic Interaction with Virtual Environemnts". IEEE Trans. Robot. Automat., Vol. 15, 465-474, June 1999.

35. Arioui, H., Mammar, S. and Hamel, T. "Master-model based time-delayed force feedback interaction: Experimental Results", Proceedings of the 2002 IEEE

International Symposium on Intelligent Control, Vancover, Canada, Oct. 27-30, 2002.

36. Cavusoglu, M. C.; Feygin, D.; Frank Tendick, F.; "A Critical Study of the Mechanical and Electrical Properties of the PHANToMTM Haptic Interface and Improvements for High Performance Control". Presence,Vol. 11. No. 6, December 2002.
37. Cavusoglu, M.C.; Feygin, D.; "Kinematics and Dynamics of Phantom(TM) Model 1.5 Haptic Interface", Technical report, 2001.
38. Niemeyer, G. and Slotine, J. E., "Stable adaptive tele-operation", IEEE Journal of Oceanic Engineering, Vol. 16, No.1, Jan. 1991.
39. Tanner, N. A.; Niemeyer, G.; "Practical Limitations of Wave Variable Controllers in Tele-operation", Telerobotics Lab, Stanford University. Technical report, 2001.
40. Slotine, J. E. and Li, W. "Applied Nonlinear Control", Prentice Hall. 1991.
41. Park, J. H. and Cho, H. C.; "Sliding-Mode controller for bilateral tele-operation with varying time delay", Proceedings of the 1999 IEEE/ASME International
42. Gopalswamy, A. and Hedrick, J. Karl, "Tracking nonlinear non-minimum phase systems using sliding control", Vol. 57, no.5, 1141-1158. 1999.
43. Hall, H., "Nonlinear Systems", Prentice Hall. 1996
44. Adams, R.J.; Hannaford, B., "Control law design for haptic interfaces to virtual reality", Control Systems Technology, IEEE Transactions on, Volume: 10, Issue: 1, 3 – 13, Jan. 2002
45. Hannaford, B. and Ryu, J.; "Time-domain passivity control of haptic inerfaces", IEEE Transactions on Robotics and Automation, Vol. 18, NO. 1, Feb. 2002.

46. Niemeyer, G. and Slotine, J. E., "Designing force reflection teleoperators with large time delays to appear as virtual tools", Proceedings of the 1997 IEEE International Conference on Robotics and Automation, Albuquerque, New Mexico, Apr., 1997.

47. Niemeyer, G. and Slotine, J. E.; "Towards force-reflecting tele-operation over the internet", Proceedings of the 1998 IEEE International Conference on Robotics & Automation, Leuven, Belgium May, 1998.

48. Goto, A., Inoue, R., "A research on tele-operation using virtual reality", IEEE International Workshop on Robot and Human Communication, 147-387, 2002.

49. Ando, N.; Korondi, P.; Hashimoto, H.; "Development of micromanipulator and haptic interface for networked micromanipulation", IEEE/ASME Transactions on Mechatronics, Volume: 6, Issue: 4, 417 – 427, Dec. 2001.

50. Colgate,J.E.; Grafing, P.E.; Stanley, M.C.; Schenkel, G.; "Implementation of stiff virtual walls in force-reflecting interfaces" Virtual Reality Annual International Symposium, 1993., 1993 IEEE , 18-22 Sept. 1993

51. Elhajj, I.; Xi, N.; Fung, W.K.; Liu, Y.H.; Hasegawa, Y.; Fukuda, T., "Modeling and control of Internet based cooperative tele-operation", ICRA Proceedings on Robotics and Automation. IEEE International Conference on , Volume: 1 , 662 – 667, 2001.

52. Elhajj, I.; Xi, N.; Yun-Hui Liu; "Real-time control of Internet based tele-operation with force reflection", Proceedings of ICRA '00. IEEE International Conference on Robotics and Automation, Volume: 4, 3284 – 3289, 24-28 April 2000.

53. Alhalabi, M. O.; Kunifuji, S. "An experimental study on the effects of network delay in cooperative shared haptic virtual environment", Computers & Graphics 27, 201-213, 2003.

54. Aghili, F., Dupuis, E. and Piedboeuf, J-C; "Force/moment accommodation control for tele-operated manipulators performing contact tasks in stiff environment", Proceedings of the IEEE/RSJ International Conference on Intelligent Robots and Systems Maui, 2227-2233, Hawaii, USA, Oct. 29-Nov. 03, 2001.

55. Munir, S.; "Internet based tele-operation", PH.D Thsis proposal, Georgia Institute of Technology, 2000.